

# Edgelit holography: Extending Size and Color

by

Ryder Sean Nesbitt

Bachelor of Science in Physical Sciences,  
California Polytechnic State University S.L.O., December 1991.

Submitted to the Program in Media Arts and Sciences  
School of Architecture and Planning  
in partial fulfillment of the requirements for the degree of

Master of Science in Media Arts and Sciences

at the  
Massachusetts Institute of Technology

September, 1999

Copyright Massachusetts Institute of Technology, 1999  
All Rights Reserved

Signature of the Author

---

Ryder Sean Nesbitt  
Program in Media Arts and Sciences

Certified by

---

Stephen A. Benton  
Allen Professor of Media Arts and Sciences  
Thesis Supervisor

Accepted by

---

Stephen A. Benton  
Chair  
Departmental Committee on Graduate Students  
Program in Media Arts and Sciences

# Edgelit holography: Extending Size and Color

by

Ryder Sean Nesbitt

Submitted to the Program in Media Arts and Sciences,  
School of Architecture and Planning  
August 6, 1999 in partial fulfillment of the requirements  
for the degree of

Master of Science in Media Arts and Sciences

## **Abstract**

This thesis provides details of research undertaken to determine practical methods of increasing the size and color capabilities of the edgelit hologram. Primary emphasis lies in the application of the edgelit hologram for image display purposes. However, the techniques developed here are applicable to other holographic recording techniques which utilize a steep-angled reference beam. The technical issues involved with edgelit holography using a glass block recording method with DuPont photopolymer recording materials are described. The considerations and procedures for scaling the size of the edgelit hologram up to 20.3 x 25.5 cm (8 x10 in) (400% larger than previously demonstrated) are given. Collimated reference beam, and phase-conjugate illumination techniques are used to record transfer images of three-dimensional objects in two steps, and techniques for obtaining true-color holographic diffusers are described. Finally, a coupled H1-H1 edgelit hologram recording method is described which has potential applications for the mass-production of holographic diffusers and stereograms.

Thesis Supervisor: Stephen A. Benton  
Title: Allen Professor of Media Arts and Sciences

# Thesis Readers

---

Michael Halle Ph.D.  
Instructor of Radiology  
Harvard Medical School

---

Joseph Jacobson  
Assistant Professor  
MIT Media Laboratory

# Acknowledgements

First I want to give thanks to Doctor-Professor Stephen Benton for allowing me the opportunity to come to the Media Lab to practice my art and learn his. Thanks to the faculty, sponsors (The Digital Life Consortium), students of the Media Lab, the Spatial Imaging Group, and especially my thesis readers Mike Halle and Joseph Jacobson. I owe thanks to Jim Gibb, for offering me that summer job working amongst those big, deep dichromates and that beautiful blue laser; and for his willingness to help out with this work. It will be real hard to repay everything--but I'm working on it. To Craig Newswanger for his willingness to teach and allowing me to learn; Sally Weber, Craig's "better half," for her encouragement and introduction to Sabrina Birner, who was instrumental in motivating me into MIT life, and inspired me to pursue edgelit work; to Wendy Plesniak, for reminding me what it was I really wanted to accomplish here; Mitch, for welcoming me to Cambridge; Dina Olivina Freedman, for her constant provocation, and trouble; Nyssim for reality checks; Lorin Wilde and Elroy Pearson for editing help; Dave Arguelles, for helping me push the envelope, and design and machine the display stand. And big thanks to Rebecca, for patience. Finally, I want to thank my Mom, who taught me that I can achieve whatever I want in life.

# Contents

<b>1</b>	<b>Introduction</b>	<b>11</b>
<b>2</b>	<b>Background</b>	<b>13</b>
2.1	Seminal work in display holography . . . . .	13
2.1.1	Transmission holography . . . . .	14
2.1.2	Reflection holography . . . . .	15
2.1.3	Edgelit holography . . . . .	15
2.2	Comparison of display hologram types . . . . .	20
2.2.1	Illumination geometry . . . . .	20
2.2.2	Recording geometry . . . . .	23
2.2.3	Fringe structure . . . . .	25
2.2.4	Recording layer shrinkage . . . . .	32
2.2.5	Optical characteristics . . . . .	32
2.3	Lippmann color holography . . . . .	35
<b>3</b>	<b>Key technical issues</b>	<b>36</b>
3.1	Introduction . . . . .	36
3.2	Recording geometry selection . . . . .	36
3.3	DuPont photopolymer recording materials . . . . .	37
3.3.1	Photopolymer chemistry and recording . . . . .	37
3.3.2	Physical characteristics . . . . .	38
3.3.3	Self-induced index matching . . . . .	39
3.4	Polarization . . . . .	39
3.5	Critical angle and the inaccessible zone . . . . .	40
3.5.1	Critical angle . . . . .	40
3.5.2	The inaccessible zone . . . . .	40
3.5.3	Accessing the edgelit zone . . . . .	41
3.6	Fresnel reflections . . . . .	42
3.6.1	Law of reflection . . . . .	42
3.6.2	Fresnel equations . . . . .	42
3.6.3	Woodgrain . . . . .	45
3.7	Reference beam irradiance calculation . . . . .	45
<b>4</b>	<b>Scaling and Color: theory and practice</b>	<b>48</b>
4.1	Introduction . . . . .	48
4.2	Collimation and phase-conjugation . . . . .	49
4.2.1	Spatial and chromatic distortions . . . . .	49
4.2.2	Phase-conjugate image playback . . . . .	50
4.3	Recording block design . . . . .	50
4.3.1	Block materials options . . . . .	51
4.3.2	The display . . . . .	51

4.3.3	Illumination angle and block size calculation . . . . .	52
4.4	Reference beam irradiance and uniformity . . . . .	56
4.4.1	Irradiance distribution . . . . .	56
4.4.2	Exposure . . . . .	57
4.5	Materials handling issues . . . . .	58
4.6	Edgelit Lippmann color holography . . . . .	58
4.7	Coupled H1-H2 edgelit hologram recording . . . . .	59
<b>5</b>	<b>Experimental</b>	<b>62</b>
5.1	Introduction . . . . .	62
5.2	Laboratory procedures . . . . .	63
5.2.1	Optical setup . . . . .	63
5.2.2	Index matching . . . . .	64
5.2.3	Irradiance measurement . . . . .	65
5.2.4	Exposure and processing . . . . .	65
5.3	Scaling size . . . . .	66
5.3.1	Three-step direct playback method . . . . .	66
5.3.2	Two-step spatial distortion tests . . . . .	70
5.3.3	Two-step transfer of a three-dimensional object . . . . .	73
5.4	Lippmann color technique . . . . .	75
5.4.1	Two-color gamut edgelit hologram . . . . .	76
5.4.2	Coupled H1-H2 edgelit recording . . . . .	79
5.6	Results . . . . .	83
5.6.1	Woodgrain reduction using photopolymer . . . . .	83
5.6.2	PMMA and photopolymer incompatibility . . . . .	84
5.6.3	Scaling and collimation . . . . .	85
5.6.4	Two-step transfers via phase-conjugation . . . . .	86
5.6.5	Coupled H1-H2 edgelit recording . . . . .	86
5.6.6	Color . . . . .	87
5.6.7	Image qualification . . . . .	89
5.6.8	Summary of results . . . . .	90
<b>6</b>	<b>Conclusion</b>	<b>92</b>
	<b>Bibliography</b>	<b>95</b>

# List of Figures

2.1	Upatnieks's glass block edgelit recording geometry (reflection-mode). The reference beam directly illuminates the emulsion through the edge of the glass block. . . . .	16
2.2	Farmer <i>et al.</i> 's improved version of the immersion tank recording geometry. The size and geometry of the tank effectively moves most Fresnel reflections away from the emulsion. . . . .	17
2.3	Waveguide hologram reconstruction geometry. Undiffracted light is guided along the block via total internal reflection. . . . .	18
2.4	Typical transmission hologram display geometry. Light is modulated toward the viewer as it is transmitted through the hologram. (The hologram substrate is not shown, and angles are specified as measured in air.) . . . . .	21
2.5	Typical reflection hologram display geometry. Light is modulated toward the viewer as it is reflected off the hologram. (The hologram substrate is not shown, and angles are specified as measured in air.) . . . . .	22
2.6	Typical edgelit hologram (transmission-mode) display geometry. Light (incident at a steep angle) is modulated toward the viewer as it is transmitted through the hologram. (The hologram substrate is not shown, and angles are specified as measured in air.) . . . . .	22
2.7	Typical transmission hologram recording geometry. Reference (REF) and object (OBJ) beams illuminate the photosensitive layer from the same side. (The hologram substrate is not shown, and angles are specified as measured in air.) . . . . .	23
2.8	Typical reflection hologram recording geometry. Reference (REF) and object (OBJ) beams illuminate the photosensitive layer from opposite sides. (The hologram substrate is not shown, and angles are specified as measured in air.) . . . . .	24
2.9	Typical reflection-mode edgelit hologram recording geometry. (REF) and object (OBJ) beams illuminate the photosensitive layer from opposite sides, but at a steep angle. (The hologram substrate is not shown, and angles are specified as measured in air.) . . . . .	24
2.10	Interference fringe structure of a conventional transmission hologram. Note how the fringes are oriented more or less perpendicular to plane of the photosensitive layer. . . . .	27
2.11	Interference fringe structure of a conventional reflection hologram. Fringes	

are oriented more or less parallel to the plane of the photosensitive layer. . . . .	28
2.12 Interference fringe structure of a typical reflection-mode edgelit hologram. Fringes are oriented more or less at a 45° angle to the plane of the photo- sensitive layer. . . . .	30
2.13 Schematic of steep-angled reference beam totally reflected by an interface and the resulting spurious fringes formed, i.e., the primary, secondary and total internal reflection (TIR) fringes. . . . .	31
2.14 Plot of wavelength change ( $\Delta\lambda$ ) needed to extinguish the diffracted wave while maintaining the readout angle constant. The edgelit hologram geometry falls within the hatched area in the middle (From Leith <i>et al.</i> [23]. Angles are specified as measured within the emulsion) . . . . .	33
3.1 The inaccessible zone for a conventional in-air recording geometry using DuPont HRF-800X-001-15 photopolymer. (All angles are specified as measured within the photosensitive layer, and the substrate is not shown.) . . . .	41
3.2 Schematic of the Fresnel reflections caused by a reference (REF) beam propagating through silver-halide material coupled to a recording block. (Refraction is omitted for clarity.) . . . . .	44
3.3 Schematic of the Fresnel reflections caused by reference (REF) beam propagating through photopolymer material coupled to a recording block. (Refraction is omitted for clarity.) . . . . .	44
3.4 Schematic diagram depicting how the energy density of steep-angled ref- erence (REF) light decreases as it is spread out from area (1) to cover a larger area (2) at the film plane. . . . .	46
4.1 Schematic of collimating edgelit hologram display stand. (side view: not to scale). . . . .	52
4.2 Schematic diagram of relevant dimensions and angle for design of display and recording blocks. . . . .	54
4.3 Two-dimensional representation of a spherical wavefront emitted by a lens pinhole spatial filter (LPSF). Note: initial gaussian beam profile not shown. . . . .	57
4.4 Schematic of a typical coupled reflection-mode edgelit recording stack. The photosensitive layer is coupled to the recording block on the side nearest the object light, and reference and object beams illuminate the photosensitive layer from opposite sides. . . . .	60
4.5 Schematic of a typical coupled transmission-mode edgelit recording stack.	



	The photosensitive layer is coupled to the recording block on the side farthest from the object light. The reference and object beams illuminate the photosensitive layer from the same side. . . . .	60
4.6	Schematic of a coupled H1-H2 recording stack. The pseudoscopic real image projection of the H1 (reconstructed in phase-conjugate) acts as the object for the H2 transfer hologram. . . . .	61
5.1	Laser beam combining setup for multi-wavelength color holography. (DF--dichroic filter, and M--high energy mirror.) . . . . .	63
5.2	Coupled recording stack for a silver-halide edgelit hologram. Note that the grey glass absorbing material is coupled to three edges of the recording block. . . . .	64
5.3	Coupled recording stack for a photopolymer edgelit hologram. Note that the grey glass absorbing material is coupled to three edges of the recording block. . . . .	65
5.4	Optical setup used for recording a conventional transmission slit master (H1). (LPSF--lens-pinhole spatial filter; M--mirror; BS--beam splitter) . . . . .	67
5.5	Optical setup used for recording the intermediate full-aperture transfer (H2). (LPSF--lens-pinhole spatial filter; M--mirror; BS--beam splitter) . . . . .	68
5.6	Optical setup used for recording the transmission-mode edgelit transfer (H3). (LPSF--lens-pinhole spatial filter; M--mirror; BS--beam splitter) . . . . .	69
5.7	Optical setup used for recording a conventional transmission H1 using a digital micromirror device (DMD) to project an image onto a diffuser. (LPSF--lens-pinhole spatial filter; M--mirror; BS--beam splitter) . . . . .	71
5.8	Optical setup used to record a transmission-mode edgelit transfer (H2) of a spatial distortion test image. (LPSF--lens-pinhole spatial filter; M--mirror; BS--beam splitter) . . . . .	72
5.9	Optical setup used to record a transmission-mode edgelit hologram (H2) from a conventional transmission H1 of a three-dimensional object. (LPSF--lens-pinhole spatial filter; M--mirror; BS--beam splitter) . . . . .	74
5.10	Optical setup used to record conventional reflection H1 with two-color gamut. (LPSF--lens-pinhole spatial filter; M--mirror; BS--beam splitter) . . . . .	76
5.11	Schematic of color test image projected onto diffuser to simulate colored area of an image. . . . .	77
5.12	Schematic of the coupled recording stack used to record a conventional reflection H1 in photopolymer. . . . .	77
5.13	Optical setup used to record a color full-aperture transfer edgelit hologram	

(H2) using a conventional color reflection H1. (LPSF--lens-pinhole spatial filter; M--mirror; BS--beam splitter) . . . . .	78
5.14 Optical setup used to record a color reflection-mode edgelit master (H1). (LPSF--lens-pinhole spatial filter; M--mirror; BS--beam splitter) . . . . .	80
5.15 Optical setup used to record a reflection-mode edgelit master (H1) hologram. Note that the distance between the diffuser in-air is less than the block thickness due to the effects of refraction. (The emulsion substrate and light absorbing materials are not shown.) . . . . .	81
5.16 Detail of typical coupled recording stack used to record a transmission-mode edgelit transfer hologram (H2) using a reflection-mode edgelit H1 coupled to the same recording block. . . . .	81
5.17 Optical setup used for recording a transmission-mode edgelit hologram (H2) hologram using an edgelit reflection H1 coupled to the same recording block. (LPSF--lens-pinhole spatial filter; M--mirror; BS--beam splitter) . . . . .	82
5.18 Digital photograph of the 20 x 25 cm monochromatic two-step transfer hologram (H2) described in Section 5.5.3. The H2 was recorded using a conventional transmission master (H1) with a 10 x 25.4 cm aperture. . . . .	89

# Chapter 1

## Introduction

Application of the edgelit hologram format can solve some of the illumination problems associated with display holography. Major development of the edgelit (also known as, edge-illuminated or steep-angled) hologram technique started just over 10 years ago.

However, in terms of size and color control, the capabilities of the edgelit hologram still do not equal those of conventional reflection or transmission display holograms, so they are not generally utilized for display applications. The purpose of this research is to extend the capabilities of edgelit holography, and provide practical methodology to enable the format to become a practical tool for visualization.

During the past 35 years, the capabilities of conventional transmission and reflection display holograms have been extended to provide meaningful full-color autostereo three-dimensional visualizations of data and imagery using computer graphic and stereographic techniques. These holograms are available in sizes up to 1 x 2 meters, with 20 x 25 cm (8 x 10 inch) and 30 x 40 cm images being more common. However, even with these technical advances, holographic displays are still not widely used. Primary reasons for limited acceptance of holographic displays are their dependence on an external light source, and their susceptibility to image blur from extraneous lights in the display environment--problems which can be solved by an edgelit hologram displays.

Practical applications, and the commercial development of the edgelit hologram format are hindered by the technique's size capabilities. The largest edgelit holograms on record have been sized 10.1 x 12.7 cm (4 x 5 in) or smaller, which is too small for a range of display applications in scientific visualization or medical imaging. The primary goal of this research was to scale the size of the edgelit hologram format to at least a 20 x 25 cm (8 x 10 inch) imaging capability--this has been achieved. In addition to scaling, Lippmann color (reflection) methods have been investigated and a coupled H1-H2 edgelit hologram recording technique has been developed which may prove useful for mass-production of holographic diffusers and stereograms.

Chapter 2 provides background information about display holography and edgelit hologram research in particular. A description of the general nature of holographic imaging techniques is given, including, illumination and recording geometries, fringe structure, and optical characteristics. Chapter 3 describes key issues specific to the edgelit format and this research, including: the use of DuPont photopolymer recording materials, polarization, critical angle, Fresnel reflections, and irradiance calculation. Chapter 4 provides theoretical analysis of the problems involved with scaling and Lippmann color techniques

as applied to edgelit holography, as well as considerations for recording block design, collimation, and phase-conjugate illumination. Chapter 5 describes the experimental procedures, and the results achieved from scaling the size of the edgelit format up to 20 x 25 cm (8 x 10 inch); the applicability of Lippmann color techniques for the edgelit format; and the development of an coupled H1-H2 edgelit hologram recording technique. Finally, Chapter 6 provides some concluding remarks and suggestions for future research.

## Chapter 2

# Background

Section 2.1 is a listing of major work done in display holography with emphasis on the development of edgelit techniques for display applications. Section 2.2 provides a comparison of general characteristics between the three main types of display holograms: transmission, reflection, and edgelit. Section 2.3 provides an overview of Lippmann color holography.

### 2.1 Seminal work in display holography

There has been extensive research on other techniques related to the edgelit recording geometry such as Total Internal Reflection (TIR) and Evanescent Wave holography. For

additional information on these techniques, other documents [3, 5, 8, 15, 19] contain references on these subjects. For the purposes of this document, the author has chosen to focus on the research being developed by the scientists mentioned below.

### ***2.1.1 Transmission holography***

#### *In-Line Technique*

In 1947 Dennis Gabor invented a method of wavefront reconstruction which captures both the amplitude and phase of the light reflected by an object [12]. He named the technique “holography,” and later received the Nobel Prize for his work. The technique Gabor demonstrated is referred to as “in-line” or “on-axis,” which describes the geometry of the optical recording setup. When an on-axis image is reconstructed, however, the illumination source and the object wavefront overlap, making the image uncomfortable to view. This is one reason why on-axis holograms are not generally used for display applications.

#### *Off-Axis Technique*

In 1963 Leith and Upatnieks[23] published a paper describing “off-axis” transmission holography and, in 1964, created images for display purposes. The off-axis geometry positions the light source away from the hologram’s normal axis, allowing comfortable viewing during image playback. In their 1966 paper, Leith *et al.* [23] characterize the structure of interference fringes and describe the basic optical properties of holograms. They discuss wavelength and angular selectivity, and the effects of emulsion shrinkage, and call attention to the “inaccessible zone” where holographic recording geometries can not go when recording with a reference beam in air. Leith and Upatnieks extended holography into the realm of image display, however, it was still unavailable to the public as a visualization tool because standard transmission holograms require a monochromatic light source to correctly reconstruct imagery. When illuminated with white light, these holograms produce strong chromatic blur.

#### *Benton’s “Rainbow” Technique*

In 1969, Benton [1] invented the “Rainbow” recording technique. This technique provides

white-light viewing of off-axis transmission holograms by reducing the vertical component of the image information (thereby reducing the vertical parallax) to band-limit the chromatic blur. Benton's technique enabled the development and production of full-color, white-light-viewable transmission holograms, which fostered the growth of the embossed display hologram industry and the acceptance of holography as a visualization tool. Most display holograms used for visualization, security, and advertising utilize the rainbow technique—including embossed holograms for credit cards and packaging, and large format imagery up to 1x2 meters.

### **2.1.2      *Reflection holography***

In 1963, Yuri Denisyuk [9] discovered the reflection recording technique. This technique is essentially the same as a color photographic technique invented by Lippmann [26]. Denisyuk extended that technique by the use of laser light sources. Reflection holograms, particularly those with thick photosensitive layers, are inherently more wavelength selective (i.e., their images have less bandwidth and chromatic dispersion) than the on-axis and off-axis transmission types. This allows white-light viewing of imagery with limited chromatic blur. Reflection holograms offer full-parallax view zones, i.e., full perspective range, and their reconstruction geometry is convenient for display applications. This technique requires high-resolution recording materials and its fringe structure is susceptible to the effects of photosensitive layer shrinkage caused by processing. Recently, the availability of environmentally stable high-resolution panchromatic recording materials has enabled the production of full-color reflection display holograms of high quality.

### **2.1.3      *Edgelit holography***

The “edge illuminated,” or “edgelit,” technique was first demonstrated by Lin [25] in 1970. The difficulties of the technique (as reported by Birner[5], who describes a personal conversation with Lin), caused Lin to abandon his efforts to pursue other work. The effects of “woodgrain” (induced by Fresnel reflections) was cited as the main reason for his decision.

In the late 1980s, Upatnieks received patents [37] involving edgelit holography. He references this work in 1988 paper [38], “Compact holographic sight.” In this paper, he describes a setup which utilized a glass block edgelit geometry (Figure 2.1) for recording 10.1 x 12.7 cm (4 x 5 in) monochromatic holograms, a grating image combiner, and a laser-illuminated display device.

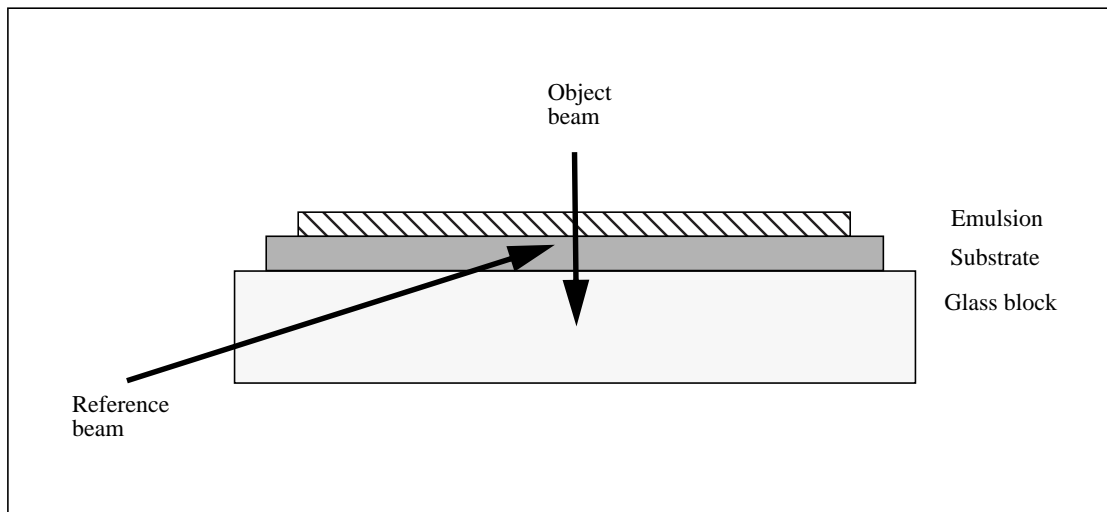


Figure 2.1: Upatnieks’s glass block edgelit recording geometry (reflection-mode).  
The reference beam directly illuminates the emulsion through the edge of the glass block.

In 1989, members of the MIT Media Lab, Benton and Birner, undertook research on edgelit display holograms. In Birner’s thesis [5], “Steep reference angle holography,” she describes many of the practical considerations of the block recording geometry. She used a glass block geometry similar to the one documented by Upatnieks, and introduced a three-step recording technique to produce the first white-light-illuminated edgelits. A 10.1 x 12.7 cm (4 x 5 in) edgelit of a three-dimensional object was demonstrated on a 2.5 cm thick Polymethylmethacrylate (PMMA) block. Recordings were made on Agfa 8E75 silver-halide plates using a He-Ne laser. A patent was later awarded to Benton and Birner [2] for a multi-color edgelit display.

In 1990, Benton *et al.* [3] reported their research on “Edge-lit rainbow holograms.”

This paper introduces an immersion tank recording geometry (Figure 2.2) which reduces the effects caused by Fresnel reflections, and discusses some of the polarization-dependent characteristics of the edgelit hologram. White-light-illuminated 10.1 x 12.7 cm (4 x 5 in) rainbow holograms were demonstrated on 1.3 cm thick PMMA blocks.

In 1991, Farmer *et al.* [10] reported their work in a paper entitled “The application of the edge-lit format to holographic stereograms.” They extended the imaging capability of edgelits to Ultragram [14] stereogram techniques and described an improved tank recording geometry. Farmer’s thesis [11], published later that year, discussed the tank recording geometry in more detail but placed major emphasis on the stereogram techniques.

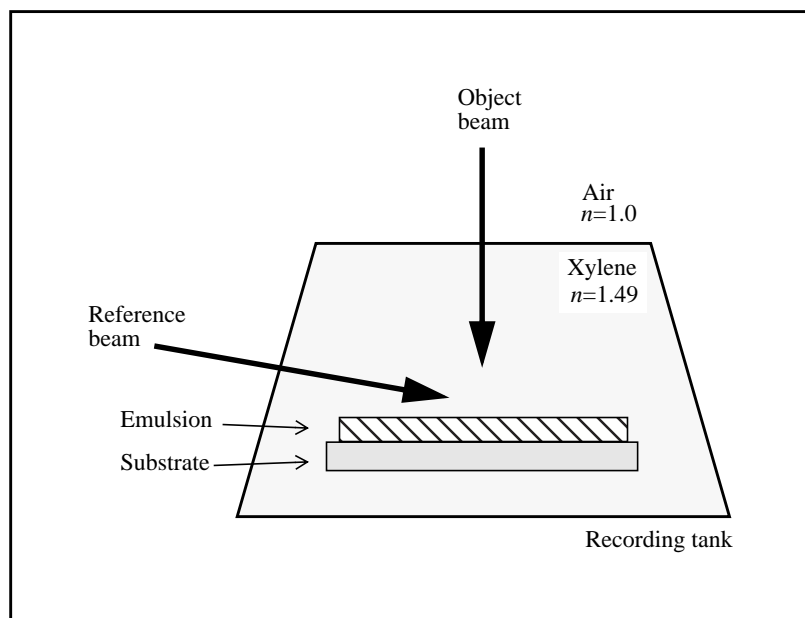


Figure 2.2: Farmer *et al.*'s improved version of the immersion tank recording geometry. The size and geometry of the tank effectively moves most Fresnel reflections away from the emulsion.

In 1991, Huang *et al.* [16] published a number of papers about waveguide holograms (WGH). Figure 2.3 below depicts a WGH and the zig-zagging of undiffracted light via total internal reflection (TIR) in the block. Huang *et al.* discuss the WGH's characteristic “multimode blurring,” which blurs deep imagery. This effect is caused by imperfect recon-



struction of the reference wavefront. They demonstrated 6.4 x 6.4 cm white-light and laser-illuminated images recorded using a block geometry (as in Figure 2.1) on Agfa 8E75 silver-halide plates using a He-Ne laser with PMMA and glass recording blocks.

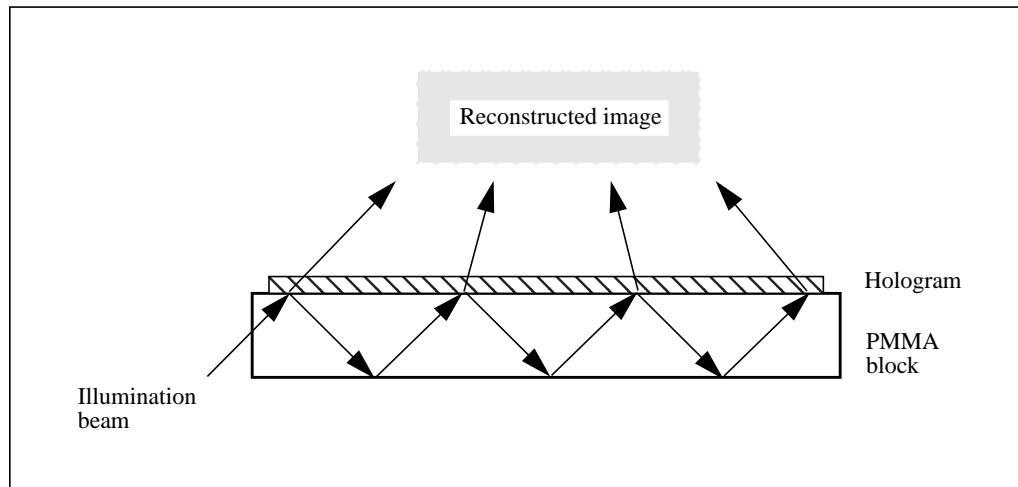


Figure 2.3: Waveguide hologram reconstruction geometry. Undiffracted light is guided along the block via total internal reflection.

A 1991 paper by Phillips *et al.*[30] gives an overview of the edgelit technique and some of the relevant issues. This paper describes a “True edge-illumination geometry” using a collimated reference beam of 514 nm light launched directly into a 2-3 mm thick photopolymer-coated glass plate with polished edges. They also give the first description of some of the promising phenomena associated with DuPont’s photopolymer recording material (Chapter 3).

Upatnieks [39] wrote another paper in 1992 elaborating on his previous edgelit paper. He lists more display and recording block geometries as well as his techniques for index matching and noise reduction. He describes using mirrors on the far surface of the block to aid beam expansion (and/or collimate the light source), and at the input end to allow for a reference beam with reduced angle of incidence. He also discusses “recycling” the undiffracted illumination light (as in the WGH above), which increases image bright-

ness, however, at the expense of image clarity.

In 1992, Kubota *et al.* [21] published “Method for reconstructing a hologram using a compact device.” They describe using an edgelit grating to collimate and introduce the reference beam into a recording block and they discuss the inter-relation between polarization and diffraction efficiency. They demonstrated a laser diode-illuminated hologram mounted to a 10 x 10 x 1 cm glass block coupled to a 1 x 1 x 10 cm illumination/collimation block. Recordings were made on Agfa 8E75 plates using a laser diode ( $\lambda = 672$  nm) source.

At a 1993 Society of Photo-Optical Instrumentation Engineers (SPIE) symposium, Henrion [15] demonstrated a 10.1 x 12.7 cm (4 x 5 in) three-color rainbow edgelit mounted onto a 1.3-cm PMMA block recorded with the Media Lab’s immersion tank using Agfa 8E75 plates and a He-Ne laser.

Also in 1993, a paper by Phillips *et al.* [31] discussed some of the materials issues involved with the edgelit’s extremely steep reference angles and the authors’ observations using DuPont’s photopolymer recording materials. In particular, they described the self-induced index matching and fluorescence characteristics of this photopolymer.

Later in 1993, Ueda *et al.* [35], in “Edge-illuminated color holograms,” described image blur of transmission and reflection-mode edgelits and mention the possibility of recording with three laser wavelengths. The authors demonstrate a 10.1 x 12.7 cm (4 x 5 in) three-color rainbow edgelit recorded on a block using Agfa 8E75 silver-halide plates and a krypton laser source ( $\lambda = 647$ nm).

In 1995, Henrion’s [15] thesis “Diffraction and exposure characteristics of the edgelit hologram,” characterized the optical properties of edgelits with an emphasis on rainbow technique. She also discusses the similarities between waveguided, evanescent, and edgelit holograms. She demonstrated 10.1 x 12.7 cm (4 x 5 in) rainbow and in-situ color [40] edgelits recorded on Agfa 8E75 plates with a He-Ne laser using the immersion tank geometry.

In 1996, Coleman *et al.* [8] published “Holograms in the extreme edge illumination geometry.” They discuss fringe structure, their transition to a direct-illumination scheme, more information about photopolymer’s effects and characteristics, and introduce a new prism recording method. In their experiments, they tested various versions of DuPont’s photopolymer materials using a krypton ( $\lambda = 647\text{nm}$ ) laser but do not describe the size of their imagery.

In 1998, Ueda *et al.* [36] published an update on their investigation into edgelit image blur. They conclude that edgelit holograms have more image blur than other types. They also recommend that transmission-mode rainbow holograms are better suited for color applications than the reflection-mode type (Section 2.2.2) in terms of image blur. Their experiments were carried out using 10.1 x 12.7 cm (4 x 5 in) silver-halide plates made with a krypton ( $\lambda = 647\text{nm}$ ) laser.

In 1998, Kihara *et al.* [18] presented their work on a “One-step edge-lit transmission holographic stereogram printer.” This effort demonstrated their conversion of Sony’s one-step printer into the edgelit mode. Monochromatic edgelits were demonstrated on 10 x 10 x 2 cm glass blocks and 5 cm diameter cylinders made using photopolymer recording materials.

## 2.2 Comparison of display hologram types

Most holographic recording methods share the basic qualities of fringe formation and recording via wavefront interference, and subsequent wavefront reconstruction via diffraction. This section provides an overview of the characteristics of conventional and edgelit display hologram types.

### 2.2.1 *Illumination geometry*

Conventional display holograms require illumination by a single distant light source with specific orientation to the hologram in order to correctly reconstruct the image for the viewer. Figures 2.4 through 2.6 depict the illumination geometries for transmission, reflection and edgelit holograms, respectively.

The illumination geometries of transmission (Figure 2.4) and reflection (Figure 2.5) holograms require a large installation area and often pose confusing logistics for people considering holograms for visualization applications. These illumination issues are major drawbacks to using conventional holographic displays in public spaces with uncontrolled lighting environments. Unless these holograms are viewed in darkened areas with controlled lighting, elaborate (and often expensive) light-blocking viewing systems may need to be used.

The edgelit hologram depicted in Figure 2.6 is illuminated by a source oriented at a very steep angle with respect to the photosensitive layer. Due to the steep-angled illumination beam, this configuration can be very compact and is unaffected by external light sources. Thus, edgelit displays can be viewed in bright, well-lit environments and in areas with limited physical space.

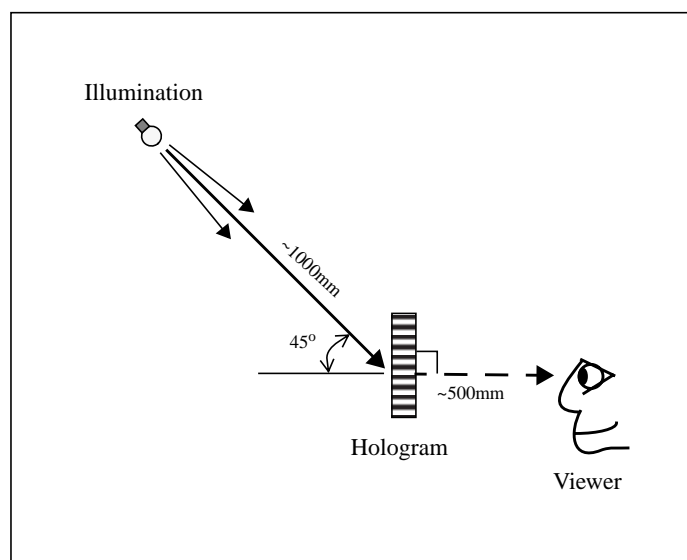


Figure 2.4: Typical transmission hologram display geometry. Light is modulated toward the viewer as it is transmitted through the hologram. (The hologram substrate is not shown, and angles are specified as measured in air.)

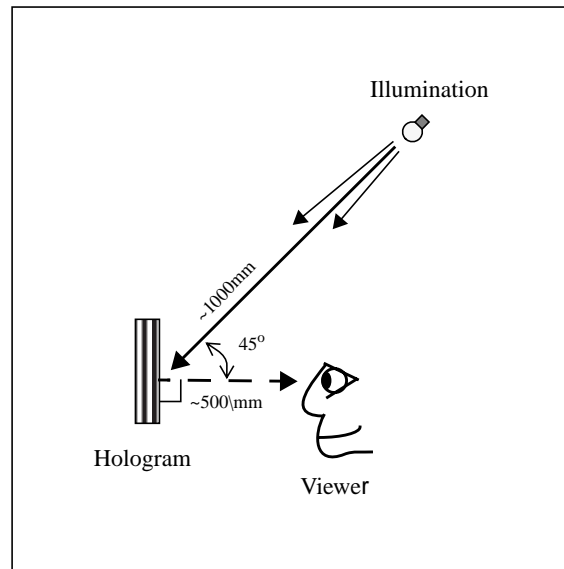


Figure 2.5: Typical reflection hologram display geometry. Light is modulated toward the viewer as it is reflected by the hologram. (The hologram substrate is not shown, and angles are specified as measured in air.)

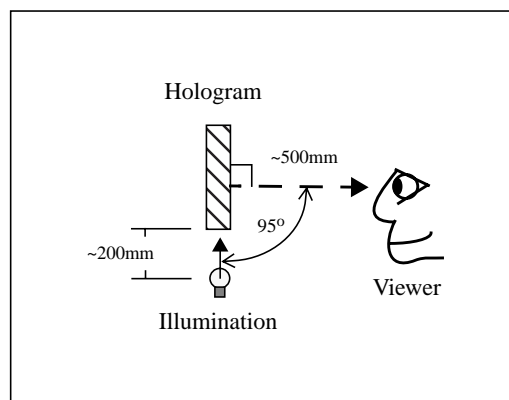


Figure 2.6: Typical edgelit hologram (transmission-mode) display geometry. Light (incident at a steep angle) is modulated toward the viewer as it is transmitted through the hologram. (The hologram substrate is not shown, and angles are specified as measured in air.)

### 2.2.2 Recording geometry

The orientation of the reference (hereafter referred to as “REF” in diagrams) wavefront with respect to the object (hereafter referred to as “OBJ” in diagrams) wavefront determines the physical parameters of the reconstruction geometry and the structure of the fringe pattern produced. The shape of the reference and object wavefronts will affect fringe structure, but the angular separation of their wavefronts is the main determinant of fringe orientation.

In the examples to follow, the object and reference wavefronts are considered collimated (located at infinity). Only one ray of light, and a small section of the recording material is depicted in diagrams for clarity. 360° angle convention is used, and object wavefronts (beams) are oriented perpendicular (0°) to the plane of the recording material (film plane) unless otherwise specified.

#### *Transmission and reflection holograms*

A transmission hologram can be recorded when the object and reference beams are coincident at the photosensitive layer from the *same* side of the plate as depicted in Figure 2.7. A reflection hologram can be recorded when the reference and object beams are coincident at the photosensitive layer from *opposite* sides of the plate as in Figure 2.8.

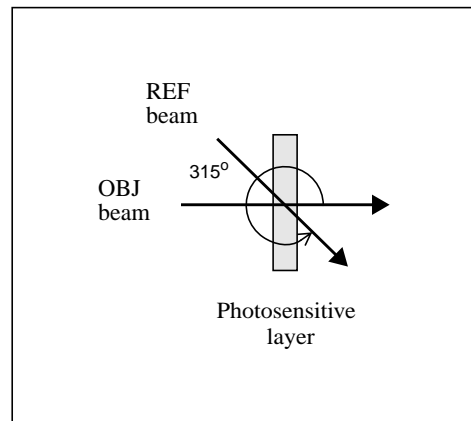


Figure 2.7: Typical transmission hologram recording geometry. Reference and object beams

illuminate the photosensitive layer from the same side.  
(The hologram substrate is not shown, and angles are specified as measured in air.)

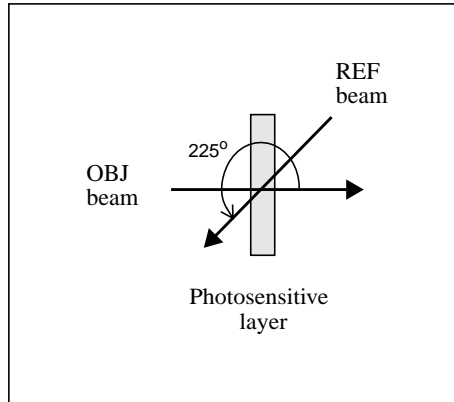


Figure 2.8: Typical reflection hologram recording geometry. Reference and object beams illuminate the photosensitive layer from opposite sides.  
(The hologram substrate is not shown, and angles are specified as measured in air.)

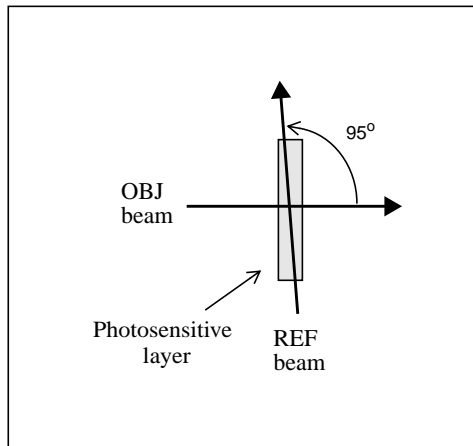


Figure 2.9: Typical reflection-mode edgelit hologram recording geometry. Reference and object beams illuminate the photosensitive layer from opposite sides, but at a steep angle.  
(The hologram substrate is not shown, and angles are specified as measured in air.)

### *Transmission-mode and reflection-mode edgelit holograms*

Figure 2.9 (above) is a schematic diagram of an edgelit recording geometry. The steep-angled reference beam of the edgelit can illuminate the photosensitive layer from either side depending on the orientation recording geometry. Thus, by the definitions above, the edgelit can be recorded as either a transmission or reflection hologram. With conventional holograms, the differences in optical characteristics of reflection and transmission holograms are very apparent and distinct (as will be shown below). However, with the edgelit hologram, the differences between the two recording modes, in terms of their optical characteristics, are slight, and reflection or transmission-mode edgelit holograms demonstrate similar optical characteristics.

#### **2.2.3 Fringe structure**

During the recording process a standing-wave interference (fringe) pattern is generated where the reference beam and object beam interfere within the recording layer. This pattern can be recorded by a high-resolution photosensitive material. The fringe pattern's orientation, or *fringe angle*, is described by the following relationship:

$$\theta_f = \frac{\theta_{OBJ-E} + \theta_{REF-E}}{2}, \quad (2.1)$$

where  $\theta_f$  is the angle at which the fringes are oriented in the photosensitive layer as measured from the perpendicular to the plane of the photosensitive layer, and  $\theta_{OBJ-E}$  and  $\theta_{REF-E}$  are the angles of the object and reference beams within the photosensitive layer.

The distance between individual irradiance peaks in the pattern, the *fringe spacing*, as measured parallel to the film plane, is described by the equation

$$d = \frac{\lambda/n}{|\sin\theta_{OBJ-E} - \sin\theta_{REF-E}|}, \quad (2.2)$$



where  $d$  is the distance between the fringes,  $\lambda$  is the recording wavelength,  $n$  is the index of refraction of the photosensitive layer, and  $\theta_{OBJ-E}$  and  $\theta_{REF-E}$  are the angles of the object and reference beams measured within the recording layer. The *spatial frequency* of the fringes is given by

$$f = \frac{1}{d}, \quad (2.3)$$

where  $f$  is the spatial frequency in cycles per unit distance  $d$ .

The *perpendicular fringe spacing* which becomes important when working with fringe structures that are oriented more or less parallel to the film plane (as they are for reflection holograms) is given by

$$\frac{1}{\Lambda} = \frac{2}{\lambda/n} \sin\left(\frac{|\theta_{OBJ-E} - \theta_{REF-E}|}{2}\right), \quad (2.4)$$

where  $\Lambda$  is the perpendicular fringe spacing,  $\lambda$  is the recording wavelength,  $n$  is the index of refraction of the photosensitive layer, and  $\theta_{OBJ-E}$  and  $\theta_{REF-E}$  are recording angles of the object and reference beams within the photosensitive layer.

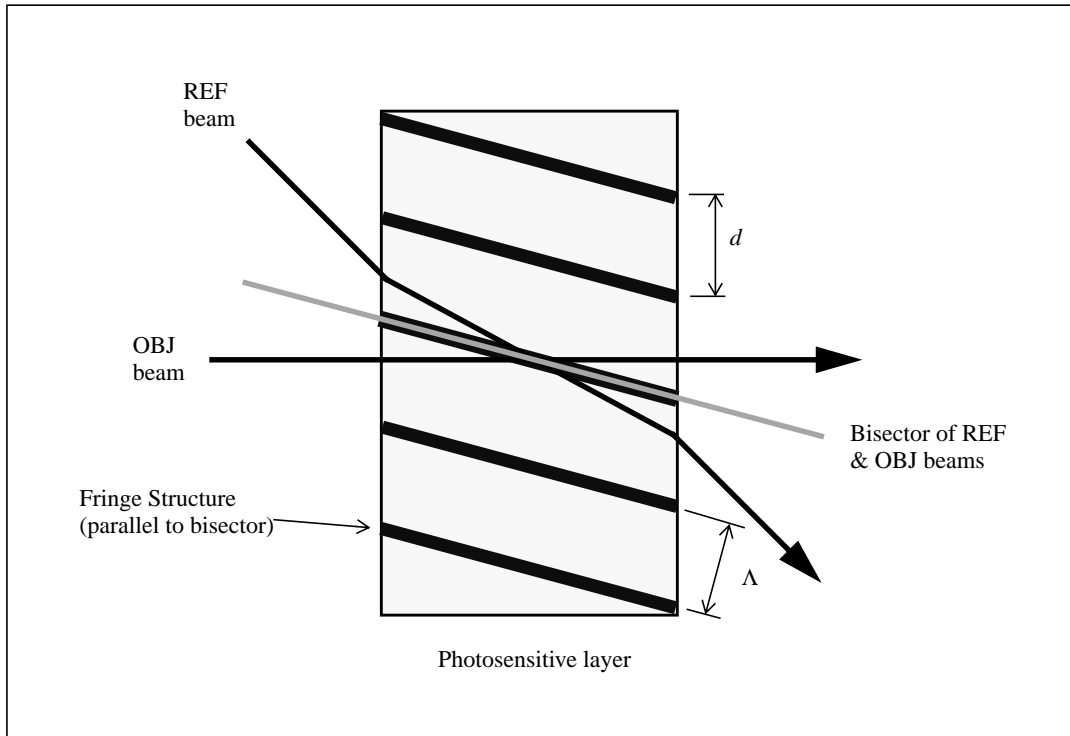


Figure 2.10: Interference fringe structure of a conventional transmission hologram. Note how the fringes are oriented more or less perpendicular to plane of the photosensitive layer.

### *Transmission holograms*

Applying Snell's law and the equations above to a typical transmission recording geometry, where  $\theta_{OBJ} = 0^\circ$ ,  $\theta_{REF} = 315^\circ$ ,  $n_{air} = 1$ ,  $n_{material} = 1.493$ , and  $\lambda_1 = 532\text{nm}$ , we determine the following:

$$\theta_{OBJ-E} = 0^\circ \text{ and } \theta_{REF-E} = 331.7^\circ; \text{ fringe angle, } \theta_f = 165.9^\circ; \text{ fringe spacing, } d = 0.75 \mu\text{m}; \text{ spatial frequency, } f = 1333 \text{ cycles/mm.}$$

Figure 2.10 above depicts the geometric orientation of a transmission hologram's fringe structure. Note how the orientation of the transmission hologram's fringe structure is more or less perpendicular to the film plane. This orientation makes the fringe structure resistant to the effects of photosensitive layer shrinkage (Section 2.2.4).

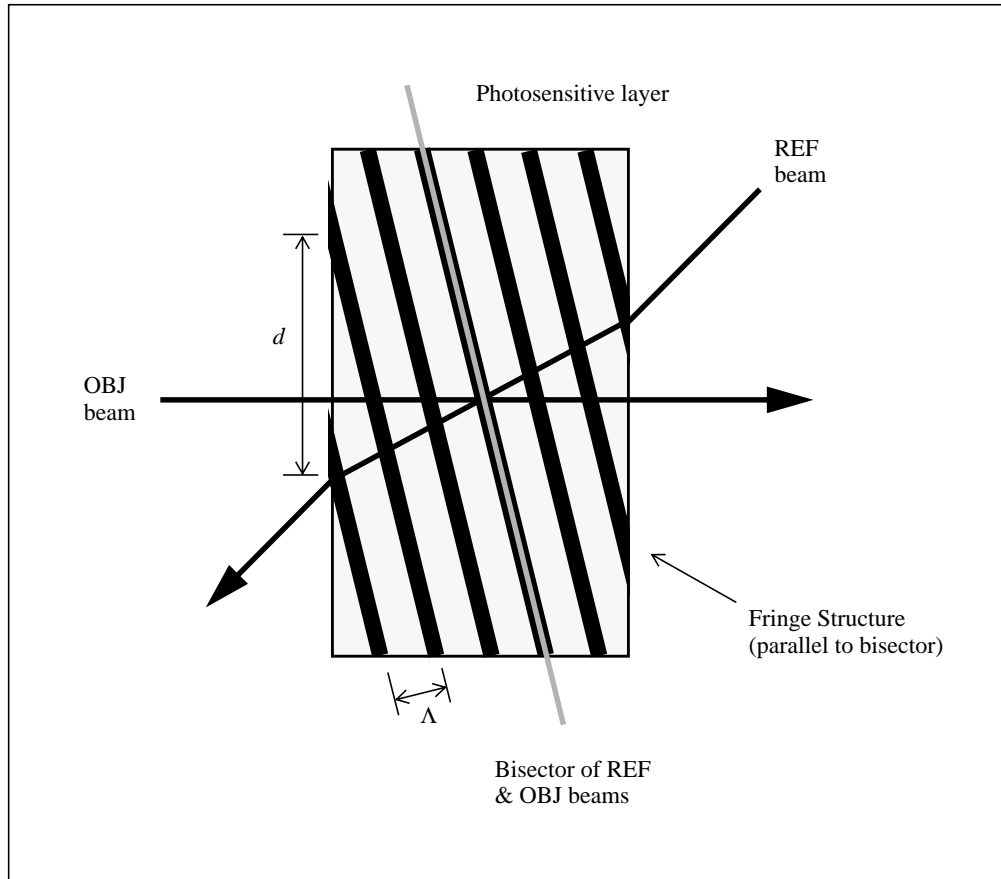


Figure 2.11: Interference fringe structure of a conventional reflection hologram. Fringes are oriented more or less parallel to the plane of the photosensitive layer.

### *Reflection holograms*

Applying Snell's law and the equations above to a typical reflection recording geometry, where  $\theta_{OBJ} = 0^\circ$ ,  $\theta_{REF} = 225^\circ$ ,  $n_{air} = 1$ ,  $n_{material} = 1.493$ , and  $\lambda_1 = 532\text{nm}$ , we determine the following:

$$\theta_{OBJ-E} = 0^\circ \text{ and } \theta_{REF-E} = 208.3^\circ; \text{ fringe angle, } \theta_f = 104.2^\circ; \text{ fringe spacing, } d = 0.75 \mu\text{m} \text{ and } \Lambda = 0.18 \mu\text{m}; \text{ and spatial frequency, } f = 5464 \text{ cycles/mm.}$$

Figure 2.11 depicts the geometric orientation of a reflection hologram's fringe structure.

Note how the reflection hologram's fringes are aligned nearly parallel to the film plane. In this orientation, fringes form in layers within the thickness of the photosensitive layer. Holograms with this characteristic fringe structure are classified as having a "thick" photosensitive layer. Most transmission holograms do not qualify for this classification because their fringes are orientated nearly perpendicular to the film plane, so their fringes do not overlap very much; thus, they are usually classified as "thin" holograms. The criterion for whether a hologram is thick or thin is given by the *Q-factor* as

$$Q = \frac{2\pi\lambda_1 t}{n_1 d^2}, \quad (2.5)$$

where  $\lambda_1$  is the recording wavelength,  $t$  is the photosensitive layer thickness,  $n_1$  is the index of refraction of the material, and  $d$  is the fringe spacing. A hologram with a  $Q$  of 10 or more is considered to be thick. The optical qualities of reflection, and other "thick" holograms, are influenced by Bragg selectivity, which will be described in Section 2.2.5.

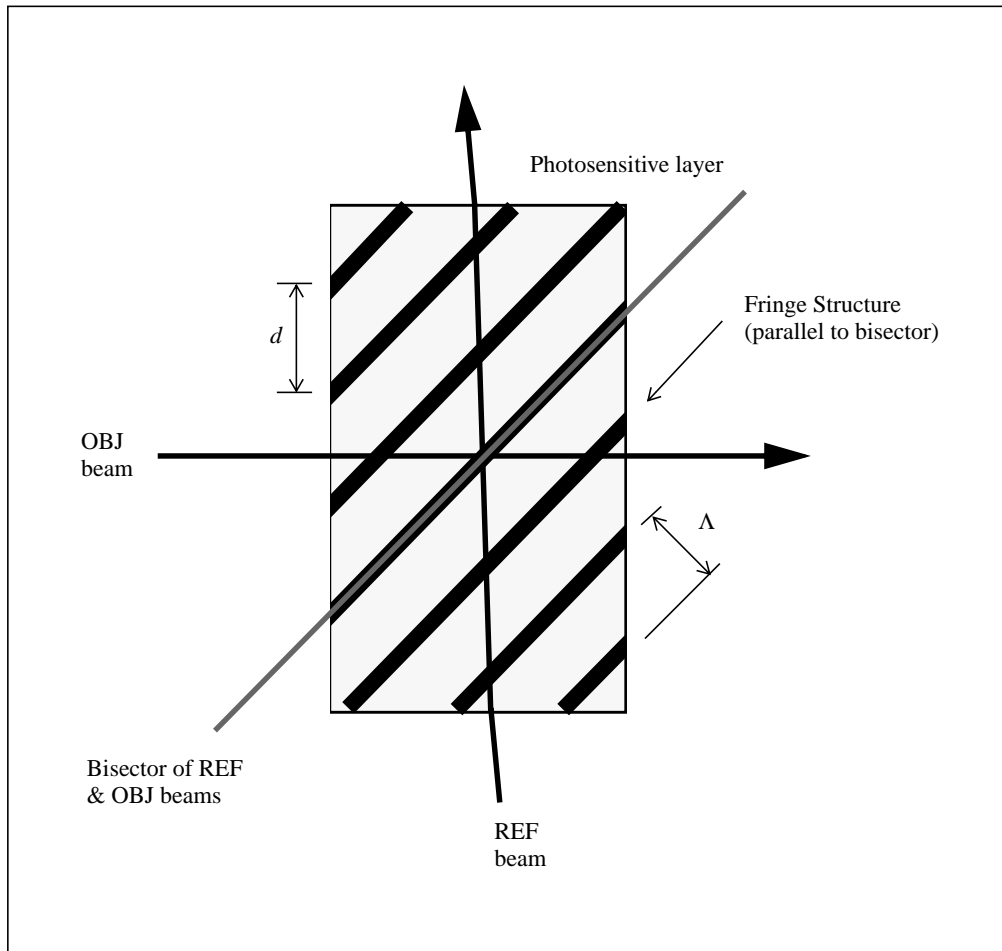


Figure 2.12: Interference fringe structure of a typical reflection-mode edgelit hologram. Fringes are oriented more or less at a  $45^\circ$  angle to the plane of the photosensitive layer.

### *Edgelit holograms*

Applying Snell's law and the equations above to a typical reflection-mode edgelit recording geometry, where  $\theta_{OBJ} = 0^\circ$ ,  $\theta_{REF} = 95^\circ$ ,  $n_{air} = 1$ ,  $n_{material} = 1.493$ ,  $t = 15 \mu\text{m}$ , and  $\lambda_1 = 532\text{nm}$ , we determine the following:

$\theta_{OBJ-E} = 0^\circ$  and  $\theta_{REF-E} = 91.7^\circ$ ; fringe angle,  $\theta_{Fringe} = 45.8^\circ$ ; fringe spacing,  $d = 0.36 \mu\text{m}$  and  $\Lambda = 0.25 \mu\text{m}$ ; and spatial frequency,  $f = 2777 \text{ cycles/mm}$ , and  $Q$ -factor;  $Q = 258$ .

Figure 2.12 depicts the geometric orientation of an edgelit hologram's fringe structure.

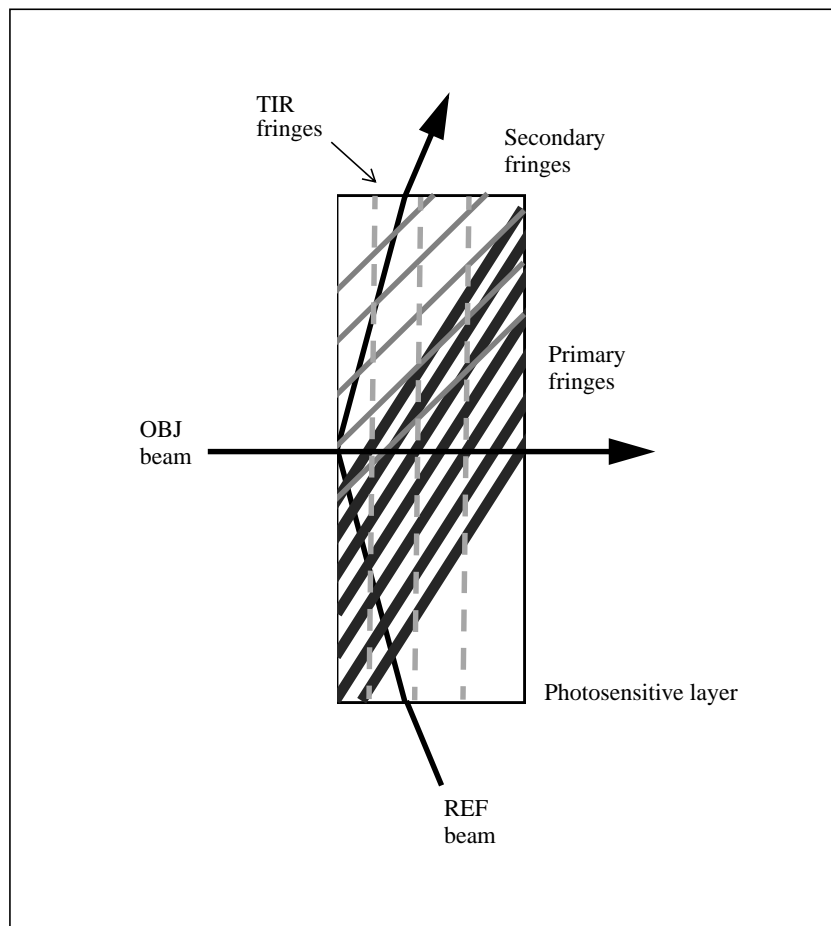


Figure 2.13: Schematic of steep-angled reference beam totally reflected by an interface and the resulting spurious fringes formed, i.e., the *primary*, *secondary* and *total internal reflection (TIR)* fringes.

### *Spurious fringes*

In reality, the edgelit hologram has a much more complicated fringe structure than described above in Figure 2.12. Edgelit recording geometries are affected by the fact that the steep-angled reference beam will eventually fall upon an interface with an index of refraction mis-match. This interface causes a Fresnel reflection of the reference which travels back through the photosensitive layer to interfere with both with the original object beam, and with the pre-reflected reference light. As shown in Figure 2.13, three separate fringe structures are formed: the *primary* set by the primary reference beam and the object beam; a *secondary* set by the totally-reflected reference beam and the object beam; and a

*total internal reflection (TIR)* set caused by the interaction of the totally-reflected reference beam with the primary reference beam.

#### **2.2.4      *Recording layer shrinkage***

Shrinkage often occurs in the recording layer when a hologram is processed. A change in the thickness of a recording layer will affect the orientation of the fringe structure [4], causing the reconstruction angle to change as well. The effects of thickness change on a fringe structure are described by the equation:

$$T_1 \cdot \tan \theta_{f1} = T_2 \cdot \tan \theta_{f2}, \quad (2.6)$$

where  $T_1$  and  $T_2$  and  $\theta_{f1}$  and  $\theta_{f2}$  are thicknesses, and fringe angles before, and after the thickness change, respectively.

#### **2.2.5      *Optical characteristics***

In the paper by Leith *et al.* [23], many of the characteristics of the edgelit hologram were predicted by extrapolating experimental data from transmission and reflection holograms into what they called the “inaccessible zone” (Section 3.5). Henrion [15] and Ueda *et al.* [36] have verified that these predictions do indeed apply to the edgelit.

##### *Wavelength selectivity (bandwidth)*

A reflection hologram formed in a “thick” photosensitive layer produces a nearly monochromatic, i.e., one-color, wavefront. This is due to the light-scattering properties of the fringe structure as described by the Bragg reflection laws. This effect is explained in more detail in other documentation [32], but a brief overview of the effect is given here.

The reflection hologram’s fringe structure is composed of layers of local index of refraction variation, filling the volume of the recording layer. The layers act as partially

reflective mirrors which change the phase of the illumination beam. Modulation of the reconstructed wavefront is achieved by way of constructive and destructive interference. Fringe structure is directly related to the wavelength used for recording. When illuminated with white light, the fringe structure acts as an interference filter, which selectively filters out wavelengths other than the recording wavelength. The image is reconstructed with a narrow band of light centered around the wavelength used for recording. This effect is called Bragg selection, and it is this selection that allows reflection holograms to be white-light viewable.

Figure 2.14 is Leith *et al.*'s [23] chart of wavelength selectivity depicting the theoretical continuity between the optical properties of reflection, edgelit and transmission holograms. The chart was calculated for a Kodak 649F emulsion coated on glass plate where  $\lambda_1 = 633\text{nm}$  and  $t = 15\mu\text{m}$ .

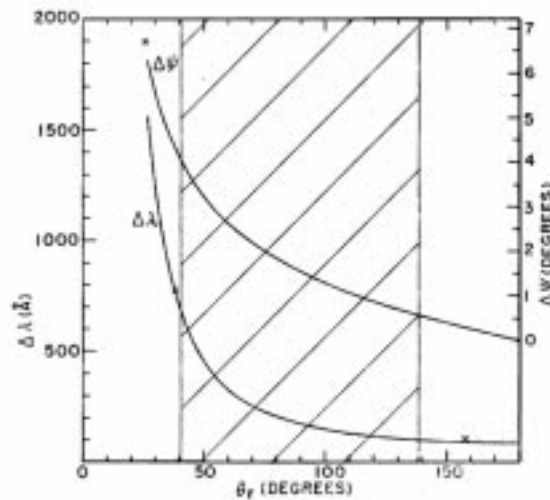


Figure 2.14: Plot of wavelength change ( $\Delta\lambda$ ) needed to extinguish the diffracted wave while maintaining the readout angle constant. The edgelit hologram geometry falls within the hatched area, the "inaccessible zone," in the middle of the chart. (From Leith *et al.* [23]. Angles are specified as measured within the emulsion)

The edgelit hologram geometry falls within the hatched region in the middle of the



graph. Thus, the edgelit hologram can display optical qualities similar to both the reflection and transmission types depending on its recording geometry. However, approximately half of the selectivity change occurs when a reference beam reaches the transmission hologram region. So on the whole, the edgelit should show qualities more like the reflection hologram. Henrion [15] confirmed this view, and her calculations of bandwidth for an edgelit, using Agfa 8E75 plates, where  $\lambda_1 = 633\text{nm}$  and  $t = 7\mu\text{m}$ , are given below in Table 1 for reference.

Table 1: Bandwidth of conventional and edgelit holograms (from Henrion [15])

Hologram type	REF angle (emulsion)	Approximate bandwidth
Conventional transmission	$25.7^\circ$	354 nm
Transmission-mode edgelit	$64.7^\circ$	61 nm
Reflection-mode edgelit	$115.3^\circ$	25 nm
Conventional reflection	$154.3^\circ$	18 nm

#### *Angular selectivity*

Leith *et al.* [23] also predicted angular selectivity for reflection and transmission holograms. Henrion [15] and Ueda *et al.* [36] have confirmed that these results apply to the edgelit as well. At steeper reference angles, holograms become more angularly selective. Overall, angular selectivity varies from  $11^\circ$  to  $2.5^\circ$ . However, in the edgelit region, selectivity nears its highest value, with a variation of only one degree.

## 2.3 Lippmann color holography

Various researchers [7, 17,20, 24, 27, 33, 36, 41] have documented methods for recording conventional color reflection holograms using the Lippmann method. With the advent of panchromatic holographic recording materials, mixed wavelength recording methods have now become possible.

As described in Section 2.2.5, reflection holograms are more wavelength selective than transmission holograms, thus, even with white-light illumination a nearly monochromatic image can be played back by the hologram. The reconstructed images of three primary-color monochromatic holograms can be mixed to obtain a natural or true-color image.

Using a multi-wavelength Lippmann holography technique, the interference patterns of mutually incoherent primary color lasers can be simultaneously recorded in a panchromatic photosensitive layer. The colors used for recording, and relative irradiance of each determine the hue and shade of the colors in the image.

# Chapter 3

## Key technical issues

### 3.1 Introduction

In this chapter, the key technical issues of edgelit holography in general are introduced. With conventional display holography, many of these issues are of no apparent consequence, but in edgelit holography, they become crucial. The focus of this section is on the practical issues specific to making edgelit holograms. For more general information on holographic production issues, the reader is advised to refer to a general holographic reference [32]. Most of the mathematics used in this Chapter assumes the materials involved (photosensitive layers and substrates) are smooth, lossless, isotropic, homogeneous dielectric media.

### 3.2 Recording geometry selection

The immersion tank geometry, designed by Farmer [10] (Figure 2.2) at the Media Lab was conceived as a method of reducing the spurious Fresnel reflections (Figure 2.13) which

previously afflicted block-recorded edgelit holograms. The tank does an excellent job of reducing Fresnel reflections, however, it is filled with volatile and flammable xylene, and becomes rather cumbersome (and hazardous) when scaled to accommodate larger holograms.

The block recording geometry is still the most often used technique [8, 16, 20, 31, 36], and provides a very vibrationally-stable recording geometry. As will be explained below, the characteristics of DuPont's photopolymer have alleviated many of the Fresnel reflection problems associated with the block recording method. For these reasons, the block recording method is investigated here.

### 3.3 DuPont photopolymer recording materials

Most of the previous edgelit research has utilized silver-halide recording materials, the properties of which, are well known and described in various literature [6, 7, 27]. Common silver-halide materials require an index matching fluid to couple the photosensitive layer to the block for recording. As will be described below, the use of index matching fluids introduces problems. DuPont's recording materials are a relatively new addition to the list of recording materials available for holography, and demonstrate advantageous characteristics when used for edgelit holography.

#### 3.3.1 *Photopolymer chemistry and recording*

As described by Stevenson [33], DuPont's photopolymer is a blend of photosensitizers and acrylic monomers dispersed in a polymeric binder material. The photosensitive layer is generally coated onto a 30 cm wide by 50  $\mu\text{m}$  thick Mylar<sup>TM</sup> polyester base substrate. Coating thicknesses are typically 15-20  $\mu\text{m}$ , and the photosensitive layer is protected by a 25  $\mu\text{m}$  Mylar<sup>TM</sup> cover sheet. The recording process takes place as follows:

When two coherent beams meet and form an interference grating in the coating layer, photopolymerization in the bright regions of the grating produce concentration gradients which drive the mobile unreacted monomers from the dark regions into the bright regions, where they polymerize. Depletion of monomer and/or vitrification eventually stops the process. The result is a permanently recorded concentration grating of photopolymer-rich regions and binder-rich regions, which form in real time during the laser exposure. This concentration grating functions as a volume phase grating when re-illuminated with a playback beam.

After exposure, the image is processed as follows: a UV light source is used to cure or “fix” the image, after which an optional baking step can be used to increase diffraction efficiency.

The recording material primarily utilized in this research was DuPont’s panchromatic HRT800X001-15 product, designed for reflection hologram production. According to DuPont [13,37], the bulk refractive index of HRF-800X001-15 is similar to their HRF-700X001 product, so those data are used here. The photosensitive layer of these materials shrinks when processed. The optical and physical properties of these materials are specified in Table 2.

Table 2: Optical and Physical Characteristics of DuPont HRF-700X001-15/HRF-800X001-15

	$n$	Thickness change, $\Delta t$
unimaged	1.493	0%
after UV	1.527	-3.8%
after Bake	1.522	-4.2%

### 3.3.2 *Physical characteristics*

The HRF-800X001-15 photopolymer material has some remarkable features which make it particularly well suited for edgelit holography. The photosensitive layer’s tacky quality

allows it to be directly laminated to the recording block, which reduces the number of interfaces that can cause Fresnel reflections (Section 3.6). However, working with film-based recording materials, especially for mastering, can be problematic, lamination, re-alignment, and flatness issues must be considered for accurate image reconstruction.

### 3.3.3 *Self-induced index matching*

As reported by Phillips [31] and Coleman [8], polymerization during the exposure process causes the index of refraction to increase in the areas where the reference (hereafter referred to as “REF” in diagrams) beam illuminates the photopolymer layer. If the index of refraction of the recording block is higher than that of the photopolymer layer, this effect can markedly reduce the interface mismatch, and increase the transmittance of the reference beam into the photosensitive layer.

## 3.4 Polarization

Lasers used for holography are generally plane polarized. Ideally, the reference and object (hereafter referred to as “OBJ” in diagrams) beams are polarized along the same axis to ensure that the fringe pattern created has the maximum possible contrast. The steep-angled reference beam of the edgelit requires close attention to the polarization angle to ensure maximum transmittance into the photosensitive layer. S-polarization (perpendicular to the plane of incidence) is desired as p-polarization (parallel to the plane of incidence) will result in low fringe contrast [3].

### *DuPont photopolymer considerations*

The photopolymer’s polyester backing substrate and cover sheet are birefringent. Birefringence causes the polarization of the light propagating through these materials to change. Care must be taken to align the optical axis of the DuPont film with that of the polarization axis of the reference beam or fringe contrast may be affected.

## 3.5 Critical angle and the inaccessible zone

### 3.5.1 Critical angle

When light leaves a medium with a low index of refraction (air) and enters a medium with a higher index of refraction (the photosensitive layer) the angle of transmittance will always be less than the angle of incidence. This relationship is expressed by Snell's law:

$$n_1 \sin \theta_1 = n_2 \sin \theta_2, \quad (3.1)$$

where  $n_1$  and  $n_2$  are the indices of refraction for the media in which the light is incident and transmitted respectively, and  $\theta_1$  and  $\theta_2$  are the angles of the incident and transmitted light.

In the case where the incident medium is the more dense media, the critical angle beyond where light can no longer penetrate the interface occurs when transmitted angle reaches  $90^\circ$ , as is given by

$$\sin \theta_c = \frac{n_2}{n_1}, \quad (3.2)$$

where  $\theta_c$  is the critical angle and  $n_1$  and  $n_2$  are the indices of refraction as described above. As long as  $\theta_1 < \theta_c$  there is only partial reflection of the incident beam. When the critical angle is exceeded ( $\theta_1 > \theta_c$ ) total reflection occurs at the interface and no light reaches the photosensitive layer (save from the evanescent wavefront [30]).

### 3.5.2 The inaccessible zone

Applying Snell's law to a conventional air/photosensitive layer interface, we find that when the angle of incidence of a reference beam in air reaches  $90^\circ$ , the critical angle in the photosensitive layer is  $42^\circ$  where,  $n_{air} = 1.0$  and  $n_{material} = 1.493$  (HRF-800X001-15 pho-

topolymer). The critical angle is significant, as it is the maximum reference angle attainable by an in-air recording techniques and imposes a limitation on fringe orientations. Leith *et al.* [23] called the regions of the photosensitive layer excluded by the critical angle (in this case, any angle over  $42^\circ$ ) the “inaccessible zone.” Figure 3.1 depicts the reference angles (specified as measured within the photosensitive layer) inaccessible to this particular air-photopolymer recording scheme.

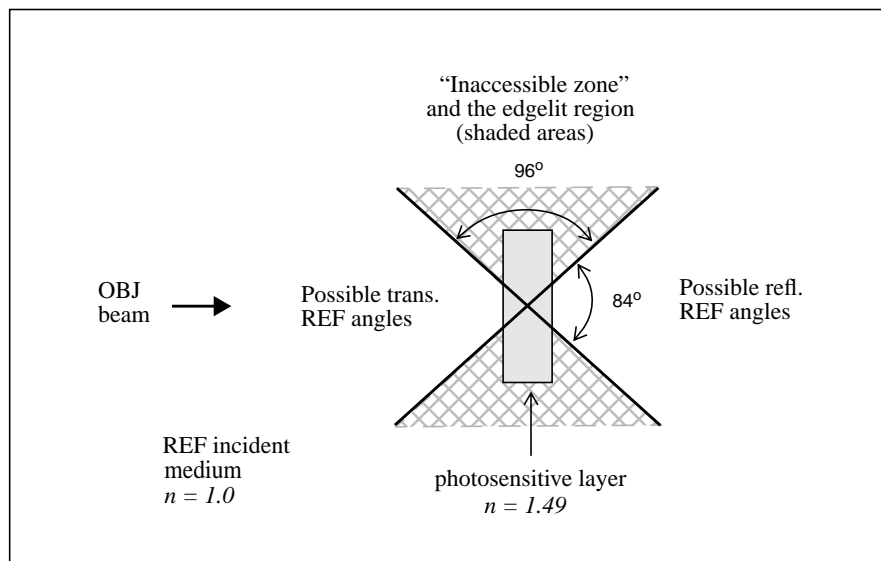


Figure 3.1: The inaccessible zone for a conventional in-air recording geometry using DuPont HRF-800X-001-15 photopolymer. (All angles are specified as measured within the photosensitive layer, and the substrate is not shown.)

### 3.5.3 Accessing the edgelit zone

By forming an interface between the photosensitive layer and incident medium with a small index of refraction mismatch, the angular extent of the inaccessible zone can be reduced and steep-angled edgelit geometries become possible. The block technique achieves this by coupling the photosensitive layer to a block of optically clear material, having an index of refraction close to that of the photosensitive layer. When a reference beam is sent through the edge of the block, the steep-angled beam can penetrate the block/



photosensitive layer interface because the index mismatch is small and the critical angle is avoided. The immersion tank geometry (Figure 2.2) is analogous to the block geometry in that it uses an intermediate material, in this case xylene instead of glass, to reduce the index of refraction mismatch between the photosensitive layer and incident medium.

## 3.6 Fresnel reflections

### 3.6.1 *Law of reflection*

Following the law of reflection and Snell's law, light impinging onto a smooth interface between two homogeneous transparent media is split into two wavefronts: one reflected and one refracted (transmitted). The law of reflection states that the angle of incidence equals the angle of reflection, that is:

$$\theta_i = \theta_r, \quad (3.3)$$

where  $\theta_i$  is the angle of incidence of the impinging wavefront, and  $\theta_r$  is the angle of the reflected wavefront. However, the Goos-Hanchen effect shows that this is not the whole story. In addition, there is a slight shift, laterally along the interface, of the reflected beam before it is reflected back into the block. However, for the purposes of this work, consideration of the Goos-Hanchen effect is not necessary, for more information, refer to Phillips [30].

### 3.6.2 *Fresnel equations*

At the steep reference angles used for the edgelit technique, the amplitudes of reflected and transmitted wavefronts become critical to the recording process as they determine the amount of light that reaches the photosensitive layer. These factors are described by the Fresnel equations as the *amplitude reflection* and *transmission coefficients*. In the case

where the laser light is polarized perpendicular to the plane on incidence (s-polarization), they are:

$$r_{\perp} \equiv \left( \frac{E_{or}}{E_{oi}} \right)_{\perp} = \frac{n_i \cos \theta_i - n_t \cos \theta_t}{n_i \cos \theta_i + n_t \cos \theta_t}, \quad (3.4)$$

and

$$t_{\perp} \equiv \left( \frac{E_{ot}}{E_{oi}} \right)_{\perp} = \frac{2n_i \cos \theta_i}{n_i \cos \theta_i + n_t \cos \theta_t}, \quad (3.5)$$

where  $r_{\perp}$  and  $t_{\perp}$  are the amplitude reflection and transmission coefficients, respectively;  $E_{or}$  and  $E_{oi}$  are the electric field amplitudes of the reflected and incident wavefronts,  $n_i$  and  $n_t$  are the indices of refraction for the incident and transmitted media, and  $\theta_i$  and  $\theta_t$  are the angles of the incident and transmitted wavefronts. Furthermore, where there is no absorption, irradiance is related to the amplitude of the electric field by the following relationship:

$$I_x = |E_x|_o^2, \quad (3.6)$$

so,

$$R_{\perp} = \left( \frac{E_{or}}{E_{oi}} \right)_{\perp}^2 = r_{\perp}^2, \quad (3.7)$$

and

$$T_{\perp} = \frac{n_t \cos \theta_t}{n_i \cos \theta_i} \left( \frac{E_{ot}}{E_{oi}} \right)_{\perp} = \left( \frac{n_t \cos \theta_t}{n_i \cos \theta_i} \right) t_{\perp}^2, \quad (3.8)$$

where  $R_{\perp}$  and  $T_{\perp}$  are the irradiance reflectance and transmittance coefficients of the perpendicularly polarized wavefronts. The other variables are the same as described above.

Figure 3.2 depicts the internal reflections caused by the coupled recording stack of a block-recorded edgelit using conventional silver-halide materials, and Figure 3.3, depicts the internal reflections produced by a coupled photopolymer recording stack.

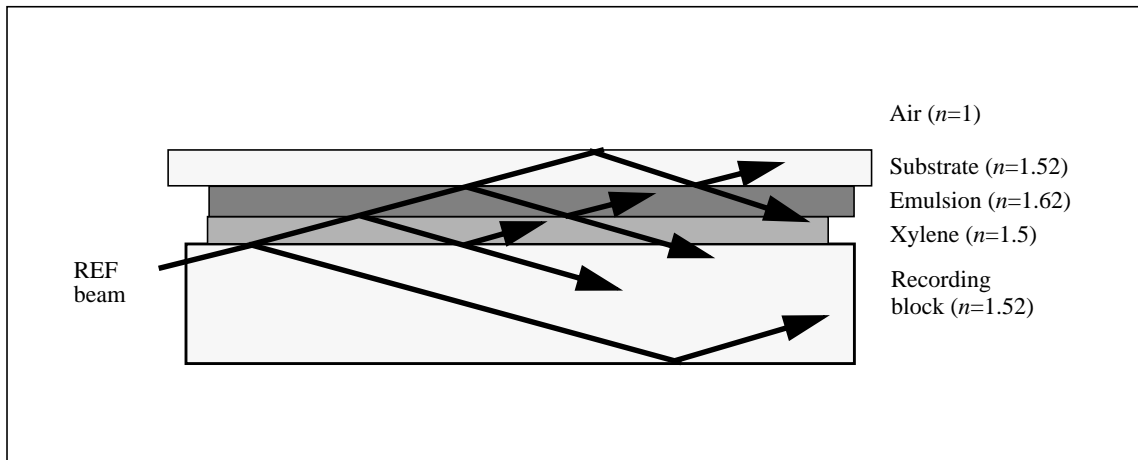


Figure 3.2: Schematic of the Fresnel reflections caused by a reference beam propagating through silver-halide material coupled to a recording block. (refraction is omitted for clarity.)

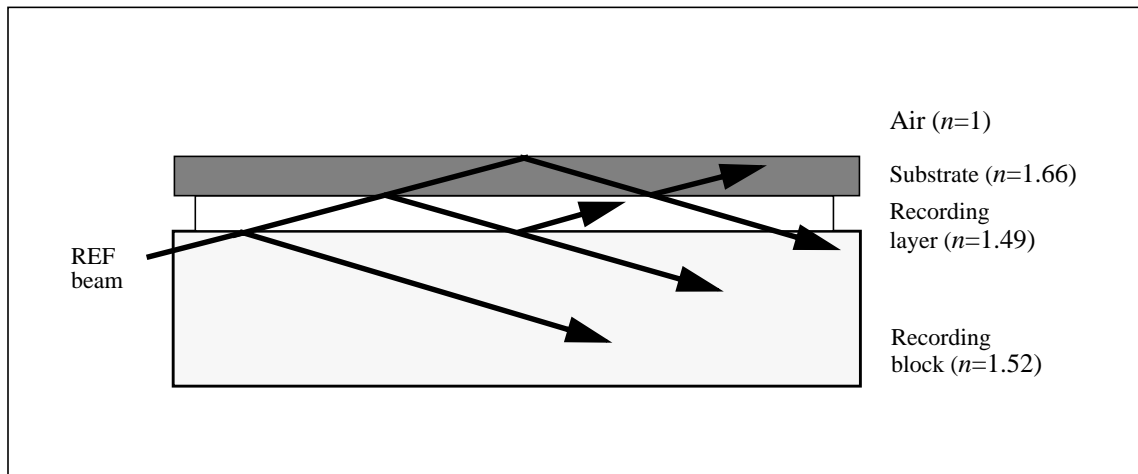


Figure 3.3: Schematic of the Fresnel reflections caused by reference beam propagating through photopolymer material coupled to a recording block. Note: refraction is omitted for clarity.

### 3.6.3 *Woodgrain*

As described above, an index of refraction mismatch between interfaces causes partial or total reflection of the incident wavefront. These spurious wavefronts interfere with each other and the reference and object wavefronts, and, due to the heterodyne effect [3], even those with low irradiance can form high contrast fringes. The more interfaces there are in the recording path, the more spurious wavefronts are formed. These fringes are generally low frequency and have a characteristic woodgrain-like appearance which is detrimental to image quality.

The primary interference pattern has to compete with these spurious interference patterns for a finite amount of dynamic range of the photosensitive material. Therefore, the presence of spurious beams in the photosensitive layer during recording reduces the overall efficiency of the hologram. If the number of interfaces and index of refraction mismatches can be reduced, woodgrain will be curtailed and the primary fringe structure will be strengthened.

#### *Attenuating woodgrain*

A method that has proven effective at reducing woodgrain for the block geometry is the index matching of light absorbing materials to the recording block. These materials must have an index of refraction nearly the same or higher than the recording block. Dark grey glass is an effective light absorber when coupled to a glass recording block with an appropriate index matching fluid. The immersion tank effectively moves the interfaces with largest index mismatch away from the photosensitive layer so that any fringes that form have a very high frequency and low irradiance.

## 3.7 Reference beam irradiance calculation

The edgelit hologram's recording geometry complicates direct measurement of reference beam irradiance for exposure calculation. The conventional irradiance measuring tech-

nique involves placing a power meter normal to the propagation vector of the incoming light near the location of the film plane. However, the steep grazing angles of the edgelit geometry cause the reference beam to undergo total internal reflection (TIR) at the air/photosensitive layer interface. Thus, there is no transmitted light to measure with the detector. To work around this problem, indirect methods are employed to measure the reference irradiance.

Birner [5] suggested index matching a diffuser to the block to view the reference light. This technique works well for evaluating the energy distribution, but does not give an accurate evaluation of the direct irradiance, which is needed for exposure calculations. Referring to Figure 3.4, we see how a steep-angled collimated reference beam passing through the narrow edge of the substrate block spreads out from an initial cross sectional area (1) to cover a much larger area (2) as it illuminates the image area. This results in lower energy density per unit area at the film plane than is measured at the input end of the block.

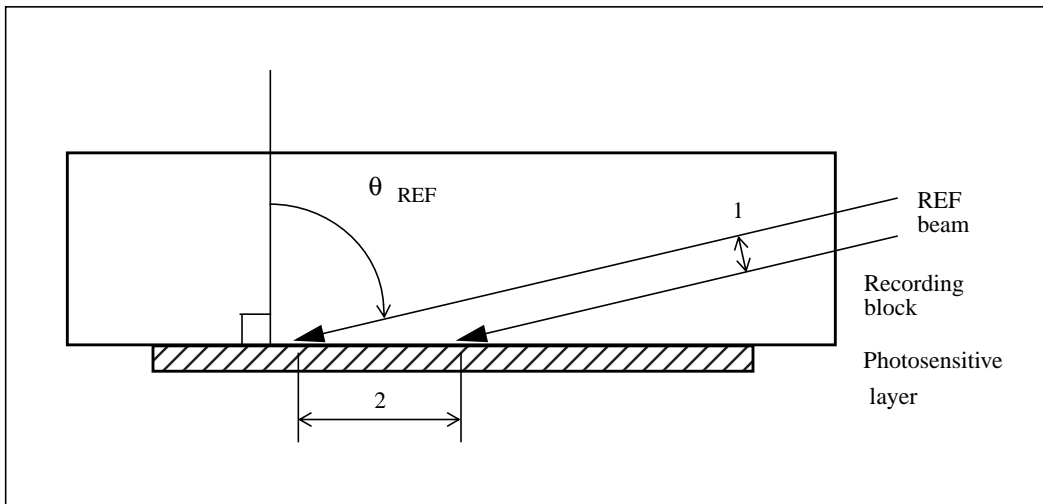


Figure 3.4: Schematic diagram depicting how the energy density of steep-angled reference light decreases as light is spread out from area (1) to cover a larger area (2) at the film plane.

To calculate the affect of a grazing angle of incidence on measured irradiance, the following equation can be used for collimated edgelit reference beams:

$$I_T = I \cos \theta_{REF}, \quad (3.9)$$

where  $I_T$  is the adjusted value for irradiance at the photosensitive layer,  $I$  is the irradiance measured at the edge of the block, and  $\theta_{REF}$  is the reference angle within the block.

At extremely steep grazing angles, Fresnel reflections become an important determinant of the irradiance reaching the photosensitive layer. For example, in the case of a block ( $n=1.516$ ) / photopolymer ( $n=1.493$ ) interface, the transmitted irradiance drops from 97% at a  $75^\circ$  (within-block) reference angle to 0% at a  $80^\circ$  (the critical angle). As long as a reference beam angle is selected that is less than the critical angle, by at least a few degrees, Equation 3.9 will suffice for most display applications.

# Chapter 4

## Scaling and Color: theory and practice

### 4.1 Introduction

In this chapter, the key issues of scaling and color control for the edgelit hologram are discussed. Solutions based on theoretical analyses are proposed to provide practical methods of integrating the edgelit format with existing recording technologies.

The considerations involved with scaling the size of the edgelit, indeed most holographic techniques, are: reference and illumination wavefront selection, display and recording setup design, wavefront irradiance and uniformity, the requirement for large beam expansion optics and higher powered lasers, and materials handling issues. In the edgelit's case some of these problems are exacerbated and more arise.

## 4.2 Collimation and phase-conjugation

Direct recording and image reconstruction using a diverging light source [2, 3, 5, 8, 10, 11, 15, 16, 31] is an effective and compact method of illuminating edgelit holograms, but it has limitations when applied to larger-sized edgelit holograms. Distortions are caused by the close proximity of the strongly-diverging source used for direct playback methods. Another drawback to this method is the requirement for an intermediate master to provide an orthoscopic real image projection to record three-dimensional objects. A collimated reference and illumination beam geometry provides solutions to these problems.

### 4.2.1 *Spatial and chromatic distortions*

In the Media Lab, and elsewhere, direct-illumination with a diverging wavefront, is the most often used method of illuminating edgelit holograms. In this method, fast (low  $f$ -number) lenses are desirable to spread out the light of the reference and illumination beams to cover the photosensitive layer in as short a distance as possible to keep the size of the display to a minimum. However, Ward *et al.* [41] noted that there are three-dimensional angular dispersion effects caused by a strongly-diverging reference wavefront located close to the hologram.

Collimated reference and illumination wavefronts should allow flexibility for slight errors in wavefront reconstruction stemming from recording layer shrinkage or imperfect phase-conjugation (which is the primary cause of these distortions). Collimation can result in less color shifting and angular deviation of image points, thus, leading to more accurate reconstruction of the image's spatial and color characteristics.

In diverging direct playback methods, the distance between the source and hologram is crucial to proper image reconstruction. If the distance is not the same as when the hologram was made, i.e., if the radius of the reconstruction wavefront is not the same as radius of the recording wavefront, spatial and chromatic distortion will occur and image quality will be affected. An ideal collimated wavefront does not diverge or converge, so as far as fringe structure is concerned, the distance between the hologram and the source does not



matter. Thus, by utilizing collimation for recording and reconstruction one source of reconstruction error and image distortion is eliminated.

#### **4.2.2 Phase-conjugate image playback**

Typical conventional two-step recording methods [4, 32] reconstruct the final transfer image using conjugate illumination (or more often, an approximation of it). Collimating the edgelit hologram's reference beam will allow phase-conjugate image playback and eliminate the need for an intermediate master hologram, thus allowing utilization of conventional two-step stereogram and three-dimensional object recording techniques.

Benton *et al.* [3] demonstrated use of a converging reference beam to achieve conjugate illumination in 10.2 x 12.7 cm (4 x 5 in) edgelit holograms. However, when scaling up to larger formats, the size of the positive lens needed to record with a converging wavefront is prohibitive, due to the physical dimensions, focal length, and expense of such an optical element. When using a collimated wavefront, the size of the collimating lens (or mirror) need only be as big as the image, or, in the edgelit hologram's case, the size of recording block's edge. Use of a phase-conjugate image reconstruction technique will require a display system which can collimate the illumination light source.

### **4.3 Recording block design**

This section outlines some considerations for designing display and recording blocks for edgelit holograms. The main considerations for block design are: hologram size, block dimensions, surface quality, hardness and index of refraction of the block material, and the reference/illumination beam geometries.

### **4.3.1 Block materials options**

#### *Polymers*

Polymethylmethacrylate (Plexiglass<sup>TM</sup>, PMMA) materials have previously [5, 16] been used as recording and display blocks. At first glance, PMMA seems attractive as a recording block because its index of refraction ( $n = 1.48-9$  [29]) is very close to that of the pre-exposed DuPont HRF-800X001-15 photopolymer recording material ( $n = 1.493$ ), but as will be shown in later chapters, other factors come into play. PMMA has good optical clarity and low birefringence compared to other plastics. However, PMMA is a relatively soft material, and its surface scratches easily.

#### *Glass*

BK-7 is an optical material which has good optical quality in visible wavelengths, and is generally available in thicknesses up to 15.25 cm. However, its index of refraction ( $n = 1.516$ ) is not an ideal match for the DuPont HRF-800X001-15 photopolymer. There are other glass types available which have a closer match to the unexposed photopolymer such as FK-5 ( $n = 1.487$ ); however, they are not readily available in large sizes and are expensive when custom made. BK-7 glass is robust and does not scratch as easily as plastic materials--making it a better choice for a recording block.

### **4.3.2 The display**

Following Snell's law (Equation 3.1), light spreads out more quickly, covering a larger area in a shorter distance, when propagating in air than in a dense medium such as glass or PMMA. To collimate the illumination light for image reconstruction, an edgelit hologram display stand (Figure 4.1) was designed that allows the illumination light to spread out before entering the display block.

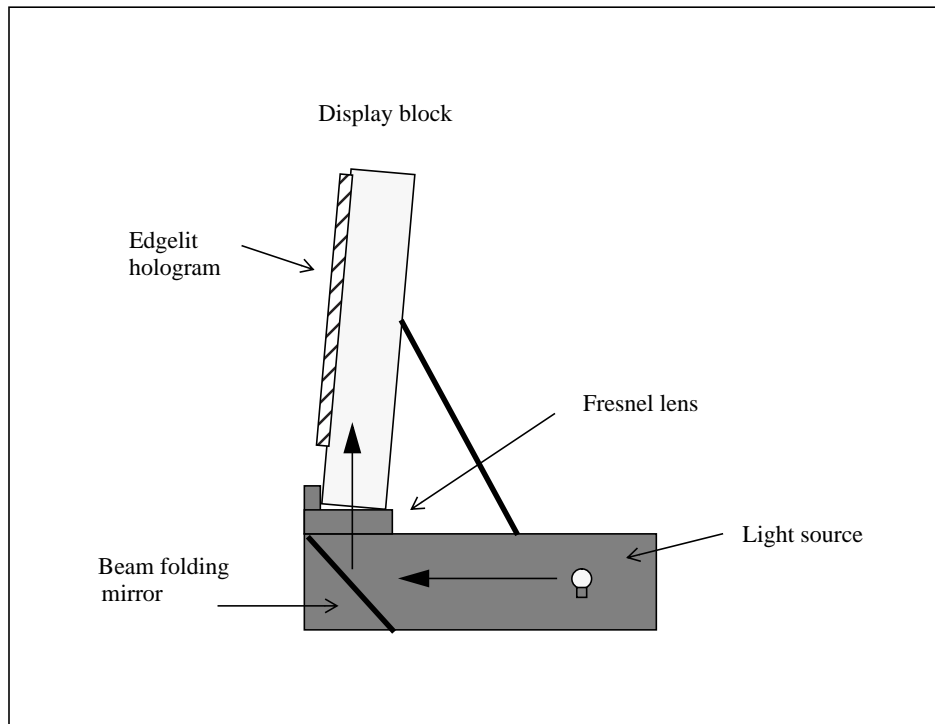


Figure 4.1: Schematic of collimating edgelit hologram display stand (side view: not to scale).

The display stand contains a 50W white-light source for broad-band illumination. A folding mirror and Fresnel lens (focal length, 21.6 cm) combination is used to collimate the light. Fresnel lenses are commonly used for overhead projector applications and are much less expensive than conventional lenses, and offer higher efficiency than most holographic optical elements. The display unit has a footprint of 25.4 x 30.5 cm, and allows adjustment of the source illumination angle to optimize image playback.

#### 4.3.3 *Illumination angle and block size calculation*

To allow for portrait or landscape illumination of medium format edgelit holograms, the geometry of the display block is designed to accommodate a 25.4 x 25.4 cm area. An additional, 5 cm area was added to the y-dimension of the block (Figure 4.2) to allow clearance

for the image and for mounting of the block to the display stand. The dimensions of the playback block were determined to be 25.4 x 30.5 x 5 cm for practicality and aesthetic reasons. These parameters are used to determine the illumination and reference angles. We begin by designing the parameters of the display itself. Then, working backward, we determine the requirements for recording the final transfer hologram.

#### *Illumination energy*

Because the index of refraction photopolymer is higher than that of the PMMA block, there is no total internal reflection (or critical angle) at this interface. However, as was shown in Section 3.7, the energy density of the light directly illuminating the photosensitive layer decreases at steeper, grazing angles due to increasing Fresnel reflection at the interface between hologram and the block. Therefore it is beneficial to reduce the illumination and reference angles as much as possible to ensure that as much light as possible can reach the hologram.

#### *Display block illumination angle*

The minimum in-block illumination angle ( $\beta_s$ ) that will allow full coverage of the photosensitive layer by a collimated beam is related to a block's dimensions by the following relationship:

$$\tan \beta_s = \frac{y}{z}, \quad (4.1)$$

where  $y$  is the length of the substrate and  $z$  its thickness. Applying this equation to the dimensions of the display block (25.4 x 30.5 x 5 cm) the minimum illumination angle is found to be  $80.5^\circ$ .

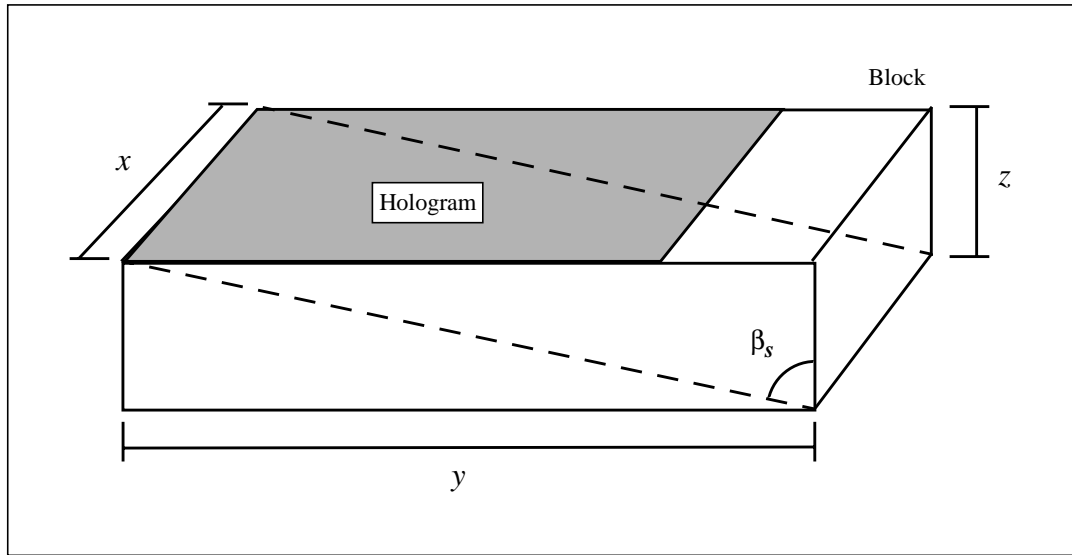


Figure 4.2: Schematic diagram of relevant dimensions and angle for design of display and recording blocks.

*Reference angle in the photosensitive layer*

Snell's law (Equation 3.1) is now applied to calculate the angle change due to refraction at the PMMA ( $n \cong 1.485$ ) / transfer adhesive (MacTac Permatrans  $n \cong 1.54$ ) interface using the illumination angle determined above ( $80.5^\circ$ ). The illumination beam angle in the adhesive is found to be  $72^\circ$ . After passing through the adhesive / Mylar<sup>TM</sup> ( $n \cong 1.66$ ) substrate interface (for phase-conjugate image reconstruction), the illumination angle in Mylar<sup>TM</sup> is found to be  $61.9^\circ$ . Next, the Mylar<sup>TM</sup> / photopolymer interface is evaluated using photopolymer's *post-bake* value for  $n$  (1.522). The illumination beam angle in the photosensitive layer is now found to be  $74.2^\circ$  (corresponding to a  $37.1^\circ$  fringe angle).

*photosensitive layer shrinkage compensation*

As described in Chapter 2, Section 2.2.3, most photosensitive layers undergo some change in thickness when processed. To pre-compensate for this effect, Equation 2.6 is applied using the post-bake thickness values given in Section 3.3, Table 2. The fringe angle is predicted to change from  $37.1^\circ$  to  $38.3^\circ$ . This change in fringe angle causes the required illumination angle to shift toward the plane of the photosensitive layer, increasing the

illumination angle from  $74.2^\circ$  to  $76.6^\circ$  (in the photosensitive layer). Simply decreasing the recording reference angle in the photosensitive layer by one degree to  $73^\circ$  in the recording setup provides an approximate solution.

#### *Reference angle in the recording block*

Now that the illumination angle ( $73^\circ$ , in photosensitive layer) that will satisfy the requirements of the display has been determined, Snell's law can again be applied to obtain the reference angle in the recording block needed to make this hologram. The photosensitive layer's *pre-exposed* value of  $n$  (1.493), the illumination angle calculated above ( $73^\circ$ ), and the index of refraction for BK-7 (1.516) are used to find the effect of refraction at the photosensitive layer/recording block interface and determine reference angle in the recording block. This angle is found to be  $70^\circ$ .

#### *Recording block thickness*

Applying Equation 4.1 to the reference angle ( $70^\circ$ ) in the recording block, we can now determine the minimum thickness of the recording block. To provide for a 20.3 x 25.4 cm image, a 28 cm high image area (in the  $y$ -direction) is desirable to allow extra room on the surface of the block for film application and image bleed. Using these parameters, the solution to Equation 4.1 tells us that the recording block must be at least 10.1 cm thick.

A block with dimensions of 27.9 x 35.6 x 10.5 cm was fabricated for these experiments. The major faces and minor edges were polished to 60-40 surface quality. A slight ( $<2^\circ$ ) wedge was put on the minor faces (with respect to the major faces) to increase the spatial frequency of any spurious gratings formed by total internal reflections and help reduce woodgrain effects.

## 4.4 Reference beam irradiance and uniformity

### 4.4.1 Irradiance distribution

The output of typical lasers has an energy distribution profile with a Gaussian shape, that is, the irradiance is highest at the center of the beam and decreases smoothly toward the edge. This affects holographic recording by causing a tendency to overexpose the central areas of the image and underexpose the edges.

In addition to a wavefront's Gaussian profile, the lens pinhole spatial filter (LPSF) commonly utilized to reduce non-uniformities in the reference beam's irradiance profile, emits a spherical wavefront. Irradiance,  $I$ , from a spherical light source decreases as the inverse square of the distance from the source as described by the *inverse square law*:

$$I = I_0 \frac{1}{r^2}, \quad (4.2)$$

where  $I_0$  is the irradiance of the light measured at the source and  $r$  is the distance from the source. The locations with equal irradiance define a spherical shape. This effect is portrayed in a 2D representation in Figure 4.3, and results in two things happening: light irradiance decreases with distance along the block; and the irradiance of the light striking the photosensitive layer is highest at the center near the base of the recording block and decreases from this location.

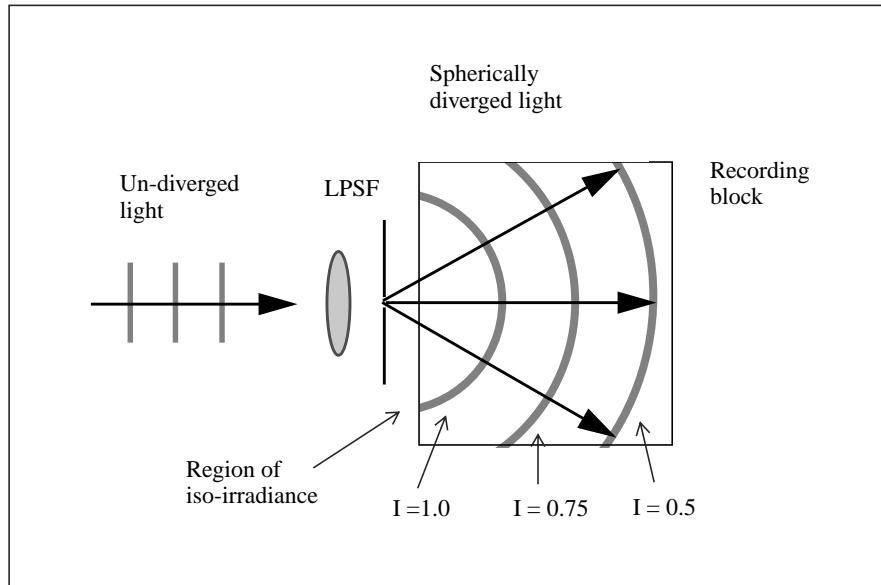


Figure 4.3: Two-dimensional representation of a spherical wavefront emitted by a lens pinhole spatial filter (LPSF). Note: initial gaussian beam profile not represented.

In conventional hologram recording techniques, large changes of reference beam irradiance can be avoided by increasing the distance between the LPSF and the photosensitive layer. As the distance from the source ( $r$ ) is increased, the loci of regions of equal irradiance become more planar--matching the film plane. This effect allows for a more even illumination of the photosensitive layer. Generation of a collimated wavefront requires the holographer to spread out the light to cover a positive collimating lens. This allows distance for the light's irradiance to even out before it enters the block.

#### 4.4.2 *Exposure*

As the reference and object beams are spread out to cover larger areas, the total energy available to expose the photosensitive layer decreases. Furthermore, DuPont's photopolymer recording materials are 50-100 times slower than the silver-halide materials previously used in edgelit research (Agfa 8E75 plates). These factors contribute to the conclusion that if photopolymer materials are going to be used with scaling up the size of



edgelit holograms, it will be necessary to use lasers with high power to avoid very long exposure times.

## 4.5 Materials handling issues

Working with a photosensitive layer on a glass substrate is the ideal way to record holograms. The glass protects and holds the photosensitive layer flat (ensuring accurate image reconstruction), and, with conventional holograms, adequately accurate index matching can be achieved using low viscosity xylene or other fluids.

On the other hand, working with thin flexible films, such as the DuPont recording materials, in medium and large format sizes is a difficult matter requiring specialized skills and patience. These materials stress easily, and, the photosensitive layer can prematurely de-laminate just by removal of the cover sheet. During lamination, bubbles, dust, and other foreign materials can find their way in between the film and the block--ruining the hologram layer and the image. The holographer usually has only one chance to get it right.

## 4.6 Edgelit Lippmann color holography

The rainbow color mixing technique, is typically used for conventional white-light transmission hologram production. Birner and Benton *et al.* [5,2,3] extended the edgelit format to the rainbow color technique. Ueda *et al.* [36] and Henrion [15] made three color edgelits using rainbow color mixing and in-situ swelling [40] techniques. Henrion reported limited availability of blue wavelengths in rainbow edgelits when using nearby diverging reference and illumination sources, which she attributed to the narrow bandwidth characteristics of the edgelit's fringe structure. Furthermore, as discussed in Section 4.2.1, the close proximity of a diverging illumination source causes three-dimensional chromatic dispersion—making color registration difficult.

Ueda *et al.* [35,36] recorded three wavelength reflection-mode edgelit holograms using three transmission masters. They concluded that rainbow techniques are better suited for edgelit holograms due to the amount of image blur inherent to the edgelit's fringe structure. They also calculated that a 30  $\mu\text{m}$  photosensitive layer thickness would be needed to obtain adequate wavelength selectivity using Lippmann color techniques. The thickness of the photopolymer materials used in this research is 15  $\mu\text{m}$ . While the thickness of this photopolymer is not as thick as Ueda *et al.* recommend, this technique is still worthy of investigation here.

## 4.7 Coupled H1-H2 edgelit hologram recording

To record a reflection-mode edgelit hologram master (H1), the recording material is coupled to the recording block as shown in Figure 4.4. This is the side of the recording block where object light would normally pass through to illuminate the photosensitive layer during the recording of a transmission-mode edgelit hologram (Figure 4.5).

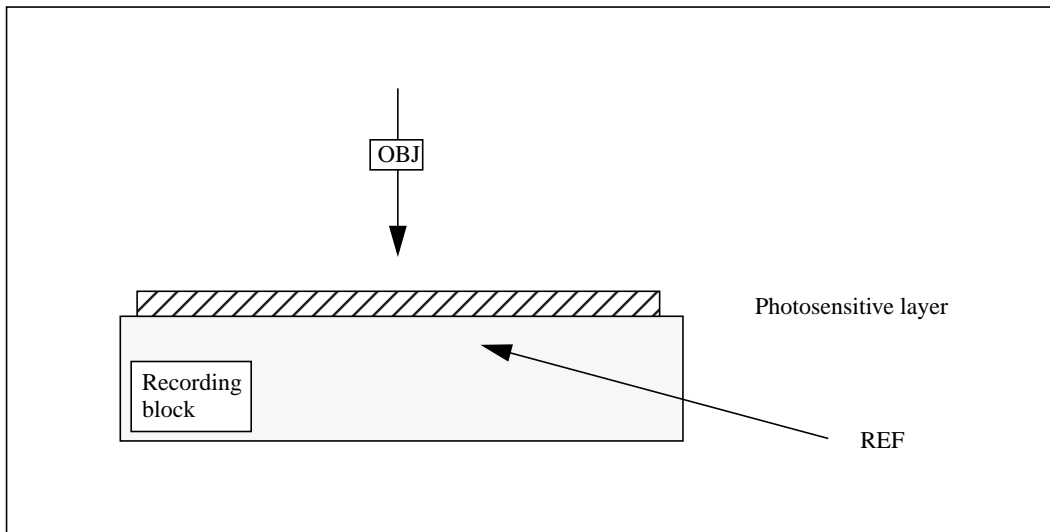


Figure 4.4: Schematic of a typical coupled reflection-mode edgelit recording stack. The photosensitive layer is coupled to the recording block on the side nearest the object light. The reference and object beams illuminate the photosensitive layer from opposite sides. (OBJ--object light, REF--reference light)

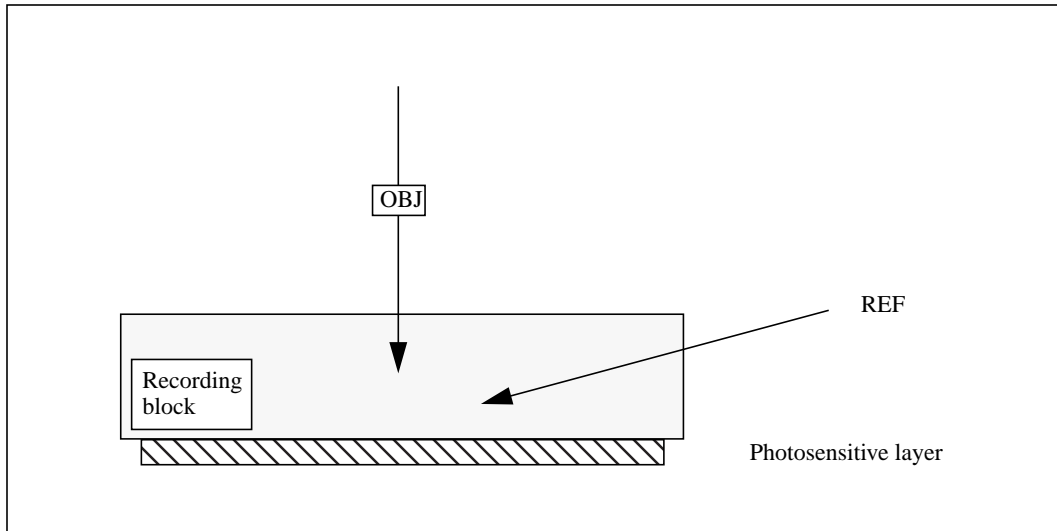


Figure 4.5: Schematic of a typical coupled transmission-mode edgelit recording stack. The photosensitive layer is coupled to the recording block on the side farthest from the object light. The reference and object beams illuminate the photosensitive layer from the same side. (OBJ--object light, REF--reference light)

If a reflection-mode edgelit H1 is made with a collimated reference beam, then coupled to the recording block for phase-conjugate illumination, its projected real image can act as the object light for a transmission-mode edgelit transfer hologram (Figure 4.6).

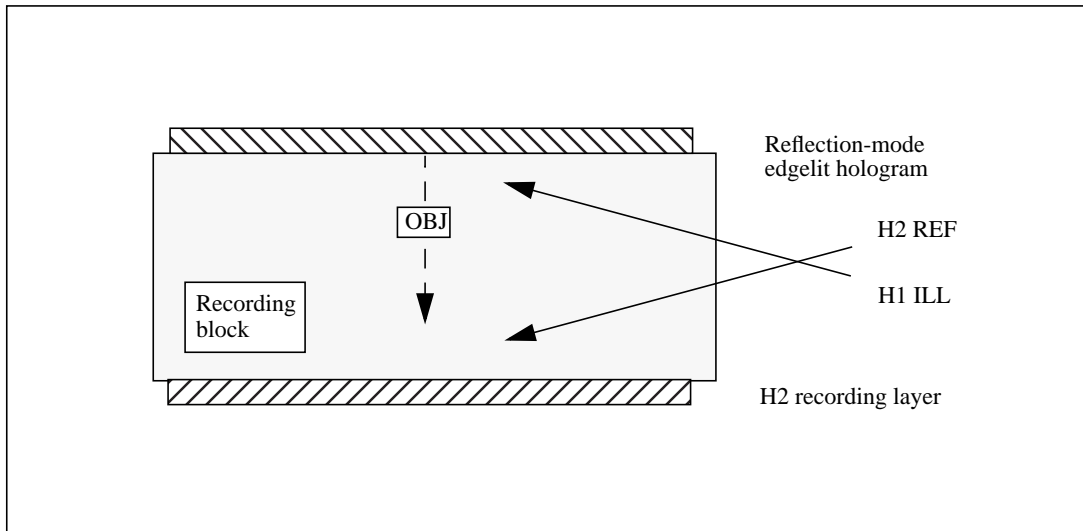


Figure 4.6: Schematic of a coupled H1-H2 recording stack. The pseudoscopic real image projection of the H1 (reconstructed in phase-conjugate) acts as the object for the H2 transfer hologram. (OBJ--object light, REF--reference light, ILL--illumination light)

This technique significantly decreases the distance between the H1 and H2, compared to the conventional method, and increases the angle of view of the image. Furthermore, the stability of the recording system is increased, as a significant part of the recording system becomes a single coupled component.

# Chapter 5

## Experimental

### 5.1 Introduction

In order to test the assertions of Chapter 4, the following experiments were undertaken. First, to gather information about the problems involved with block recording, the three-step technique developed by Birner and Benton [2,3,5] was explored. Next, scaling issues, collimation, phase-conjugation, chromatic and spatial distortions, and color were evaluated. Finally, the coupled H1-H2 edgelit recording technique was explored.

In the diagrams to follow, one may note inconsistencies in the optical setups used, i.e., a parabolic mirror that was removed from a setup for technical reasons early on, appears again in later sections. Over the course of this research, some experiments were carried out at different times, but in this document related research is located in the same section, regardless of chronology.

## 5.2 Laboratory procedures

### 5.2.1 *Optical setup*

Reference and object beam path lengths were matched to be within 1 cm when possible. Sometimes it was necessary, due to the physical constraints of the optical system, to add additional length to one of the paths. In this case, three additional mirrors were used to send the beam with shorter path additional distance to equalize the path lengths. All angles are measured with respect to the object beam.

The multi-wavelength beam combining system used for Lippmann color holography is depicted in Figure 5.1. Coherent Inc. Innova 100 argon (457 nm) and krypton (647 nm) ion lasers, and a Coherent solid-state diode Nd:YagII (532 nm) laser were used.

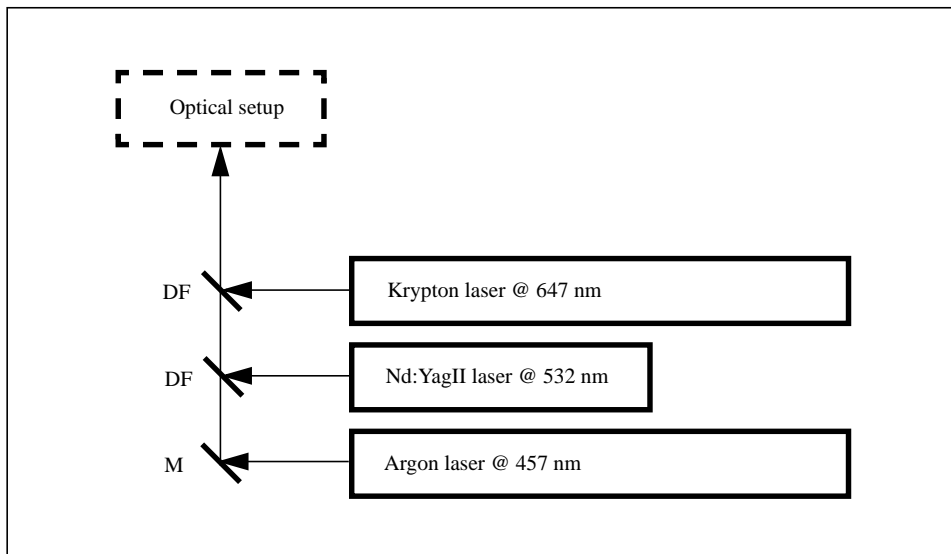


Figure 5.1: Laser beam combining setup for multi-wavelength color holography. (DF--dichroic filter, and M--high energy mirror.)

Polarization was set perpendicular to the plane of incidence (s-polarization) as measured near the film plane. Masters were aligned to satisfy their Bragg condition (measuring maximum diffraction efficiency). A settling time of at least two minutes allowed vibrations to settle prior to exposure.

### 5.2.2 *Index matching*

Conventional transmission H1s (and H2's in the three-step method) were mounted to a grey glass plate holder using xylene for recording, and then to a clear glass plate holder (again with xylene) for transfers. For edgelit hologram recording, silver-halide plates were index matched to the recording block using either xylene or Cargille immersion liquid ( $n = 1.51$ ) as depicted in Figure 5.2. DuPont photopolymer film was typically applied with the photosensitive layer toward the recording block, held by its own tackiness. The photopolymer recording stack is shown in Figure 5.3. 6.4 mm thick pieces of dark grey glass were index matched to three of the glass recording block's edges to absorb spurious light.

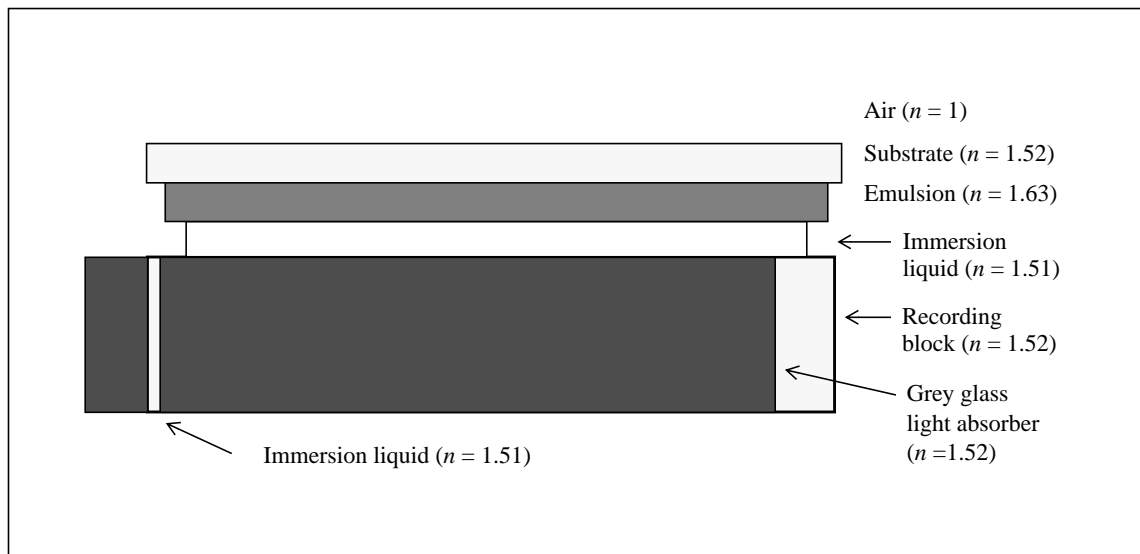


Figure 5.2: Coupled recording stack for a silver-halide edgelit hologram. Note that the grey glass absorbing material is coupled to three edges of the recording block.

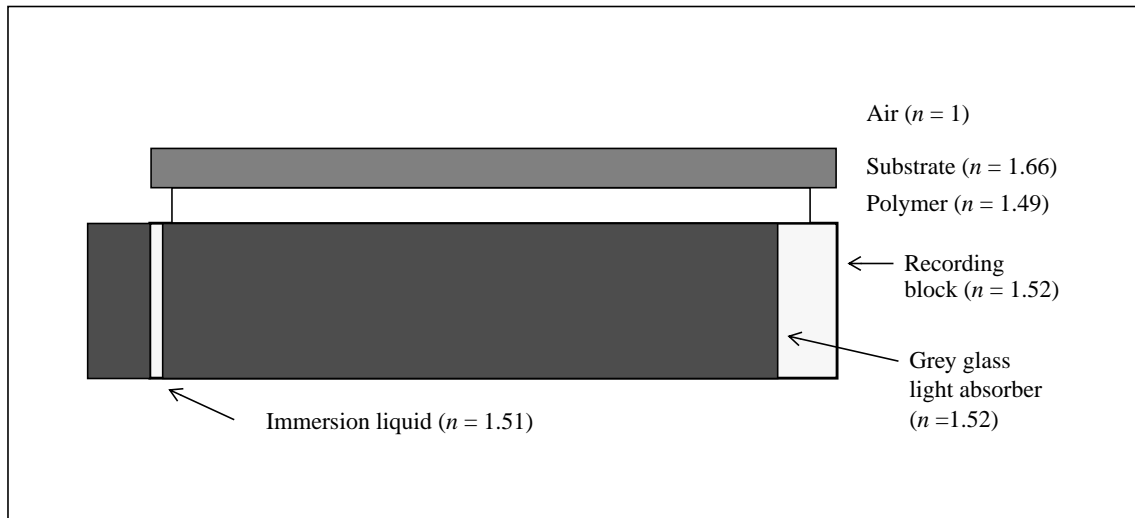


Figure 5.3: Coupled recording stack for a photopolymer edgelit hologram. Note that the grey glass absorbing material is coupled to three edges of the recording block.

### 5.2.3 Irradiance measurement

To avoid over modulation of silver-halide materials, the brightest areas of the reference and object wavefront are often used for exposure calculations. DuPont's photopolymer allows for some overexposure, but is more critical of beam ratio, so spatially-averaged irradiance values were used with photopolymer. Reference beam irradiance was measured at the block's edge and then Equation. 3.8 was applied to calculate the direct reference irradiance incident on the photosensitive layer. object beam irradiance was measured at the film plane.

### 5.2.4 Exposure and processing

#### *Silver-halide plates*

Agfa 8E56 silver-halide holographic recording plates were exposed to  $60\mu\text{J}/\text{cm}^2$  of light. Processing consisted of: Ilford two-part developer for 3 minutes; water rinse for 3 min-



utes; bleaching with EDTA (twice clearing time); water rinse for 5 minutes; and drying in graduated alcohol baths (fifty, seventy-five, and one-hundred percent concentrations).

### *Photopolymer film*

DuPont's HRF-800X001-15 coating has different film speeds for each wavelength used for recording. Exposures ranged between 2 and 3 mJ/cm<sup>2</sup> of total (R+G+B) energy. For color recordings, a 4:1:2 (R:G:B) irradiance ratio was used as a baseline. Each beam's irradiance was adjusted by controlling the laser output power to obtain the desired ratio. This allows for one exposure time which simultaneously supplies the necessary energies for all wavelengths. Reference to object beam ratios were set as close as possible to 1.5:1. Processing consisted of: a UV cure for ~45 seconds; and baking at 120°C for 2 hours.

## 5.3 Scaling size

The goal of this section is to lay the groundwork for scaling up to 20.3 x 25.4 cm edgelit holograms. Then, to evaluate any distortions introduced by the collimated reference scheme, phase-conjugate image reconstruction, or two-step mastering techniques. 532 nm laser light from a doubled-YAG laser was used for all mastering and transfer steps.

### *5.3.1 Three-step direct playback method*

Birner's thesis [5] was found to be the best introduction to the production of edgelit holograms. This document provides practical descriptions of issues and procedures for recording edgelit holograms of three-dimensional objects. To establish a base understanding of the technique, Birner's recipes for producing edgelits using the three-step recording method on silver-halide were investigated first.

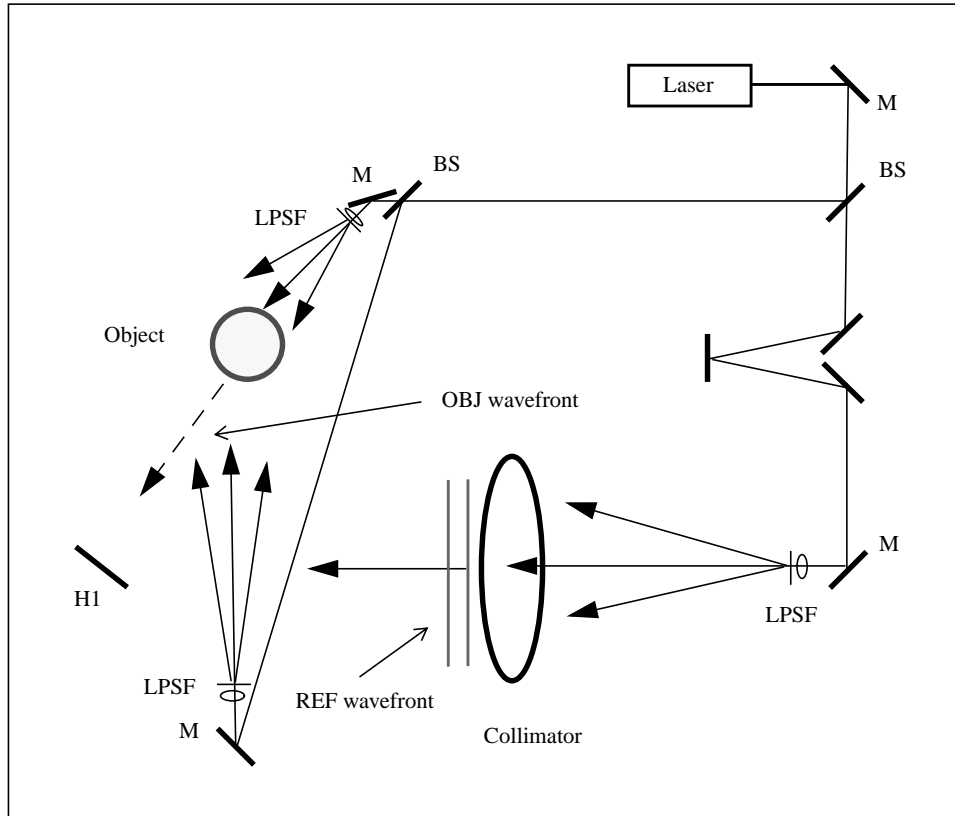


Figure 5.4: Optical setup used for recording a conventional transmission slit master (H1). (LPSF--lens-pinhole spatial filter; M--mirror; BS--beam splitter)

### *Slit master (H1)*

Figure 5.4 depicts the transmission H1 mastering setup. A bronze sculpture of a Manta Ray was mounted onto an aluminum base plate with reflective objects suggesting seaweed located at various depths around the sculpture. The total dimensions of the scene were: 22 x 30 x 20 cm. A location was picked 2.54 cm from the front of the diorama to be the final film plane location for the H3 and the primary lighting paths were matched to this location. The distance from this plane to the H1, which determines the distance from the H3 to the viewer, was 350mm. The object was top-lit for a natural appearance, and a key light was placed behind the object to obtain highlights from the Manta Ray and coral. A 5 x 25.4 cm silver-halide recording plate was illuminated with a collimated reference beam at 45° and a beam ratio of 30:1 was used.

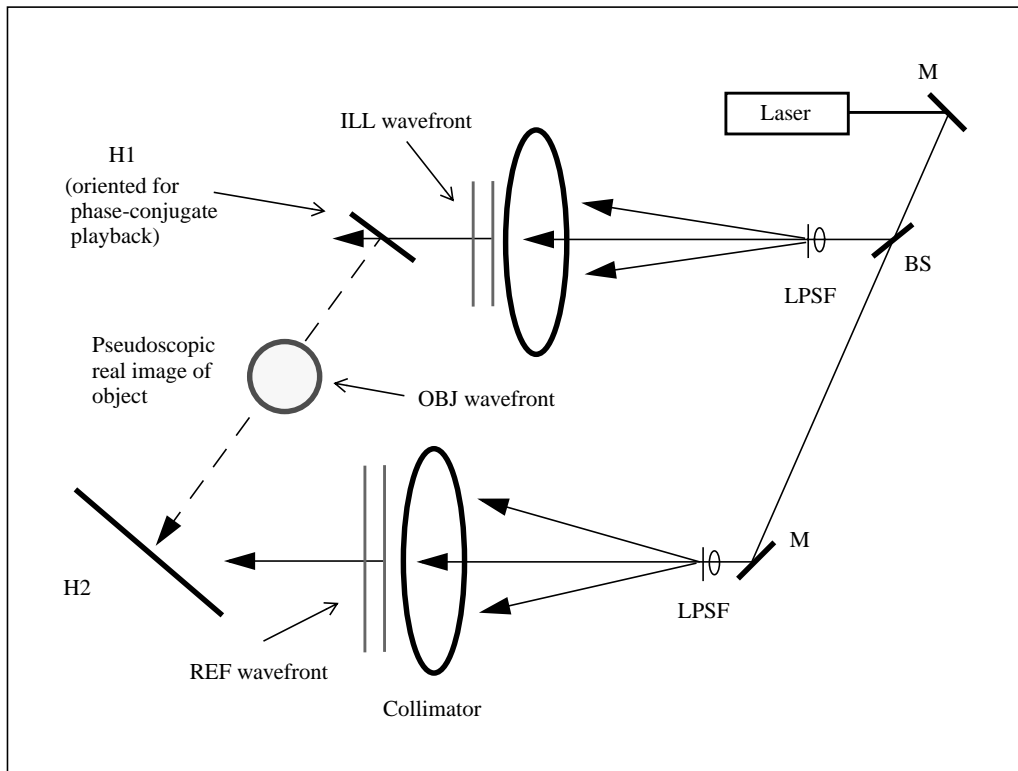


Figure 5.5: Optical setup used for recording the intermediate full-aperture transfer (H2). (LPSF--lens-pinhole spatial filter; M--mirror; BS--beam splitter)

### *Intermediate master (H2)*

Figure 5.5 above, depicts the optical setup for recording the transmission H2 later used to obtain an orthoscopic real image projection of the object. The H1 to H2 distance was set to 500mm to allow the undiffracted zero-order light from the H2's ILL beam to clear the edgelit recording block in the next step of the procedure. The H1 was orientated for conjugate image reconstruction and illuminated with collimated light. A 20.3 x 25.4 cm H2 was illuminated with collimated light at a 45° reference angle, and beam ratio of 20:1 was used.

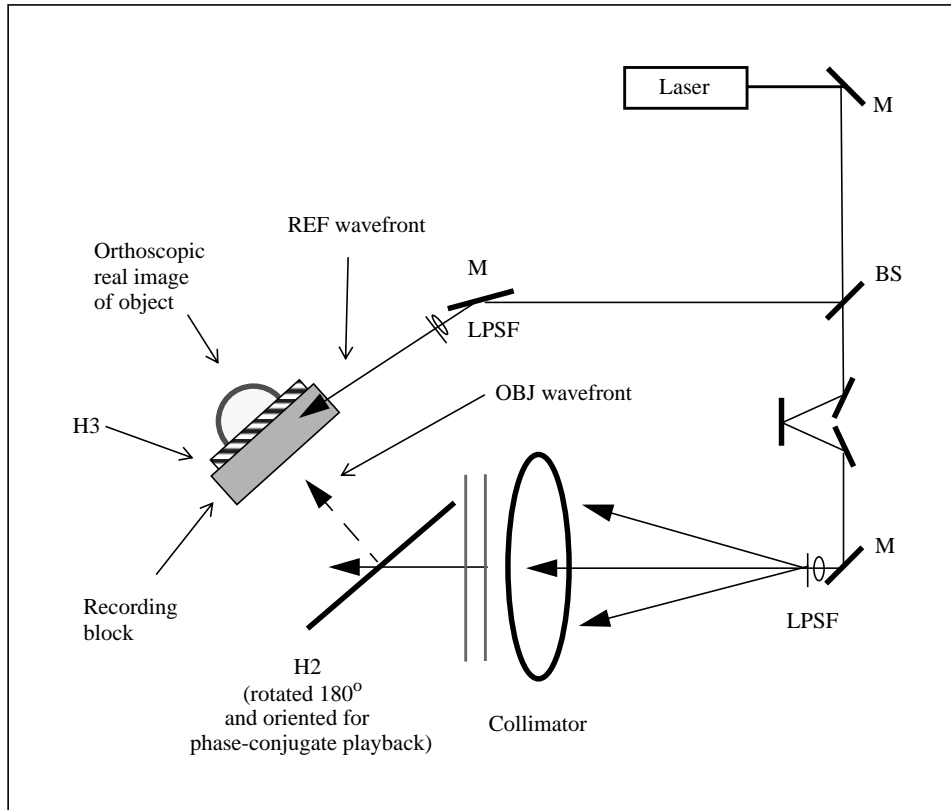


Figure 5.6: Optical setup used for recording the transmission-mode edgelit transfer (H3). (LPSF--lens-pinhole spatial filter; M--mirror; BS--beam splitter)

### *Edgelit transfer (H3)*

The optical setup for recording the edgelit transfer hologram is shown on Figure 5.6 above. The H2 was rotated 180°, oriented for conjugate playback, and illuminated with collimated light. For recording of a transmission-mode edgelit, the block was located so as to place its back surface (the surface farthest away from the object beam) at the pre-determined image plane of the object. The H3 reference beam was a diverging wavefront oriented at an in-block angle of 75° from a source located 25.4 cm from the block. The first H3 exposure tests were made using silver-halide plates and a PMMA recording block. Eventually, the PMMA block was replaced with a 25.2 x 15.2 x 5 cm BK-7 glass block, and H3 recordings were made with photopolymer. Beam ratios between 1 and 20:1 were tested.

### *Observations and discussion*

Both of the conventional transmission holograms (H1 and H2) were bright and suitable for use as masters. Edgelit transfer holograms (H3) were index matched to a PMMA block using Cargille immersion fluid ( $n = 1.51$ ) and illuminated with a broad-band white-light source for evaluation.

The silver-halide edgelit transfers (H3) recorded on PMMA immediately demonstrated the difficulty of this technique. The images had very bad woodgrain, and very little of the image information was visible. Various light absorbing materials were tested, such as dark PMMA, and dark PMMA diffusers, but nothing completely solved this problem. Edgelit (H3) holograms shot on DuPont's photopolymer immediately provided a reduction in woodgrain.

It was thought early on that PMMA would prove to be an ideal candidate as a recording block because its index of refraction is close to that of photopolymer. Thus, the PMMA block was replaced in the setup for further testing. However, satisfactory results could not be obtained using PMMA, thus, BK-7 was determined to be the material of choice, and a block suitable for recording large edgelits was fabricated.

#### **5.3.2**      *Two-step spatial distortion tests*

Most of the holographic display imagery used for visualization in the Media Lab and elsewhere is created using stereographic techniques. Conventional two-step techniques use a composite slit master hologram (H1) which is essentially a series of recordings of a flat diffuser (Halle and Saxby [14, 32] for more information on stereograms). The H1 is illuminated for phase-conjugation, and a transfer hologram (H2) is recorded of the projected real pseudoscopic image of the diffuser located near the H2 film plane. The H2 is then illuminated in phase-conjugate to reconstruct an orthoscopic image of the diffuser (normally) transferred onto the H2 film plane. Everything is much easier if the diffuser maintains its original planar shape--particularly when using the rainbow color mixing techniques.

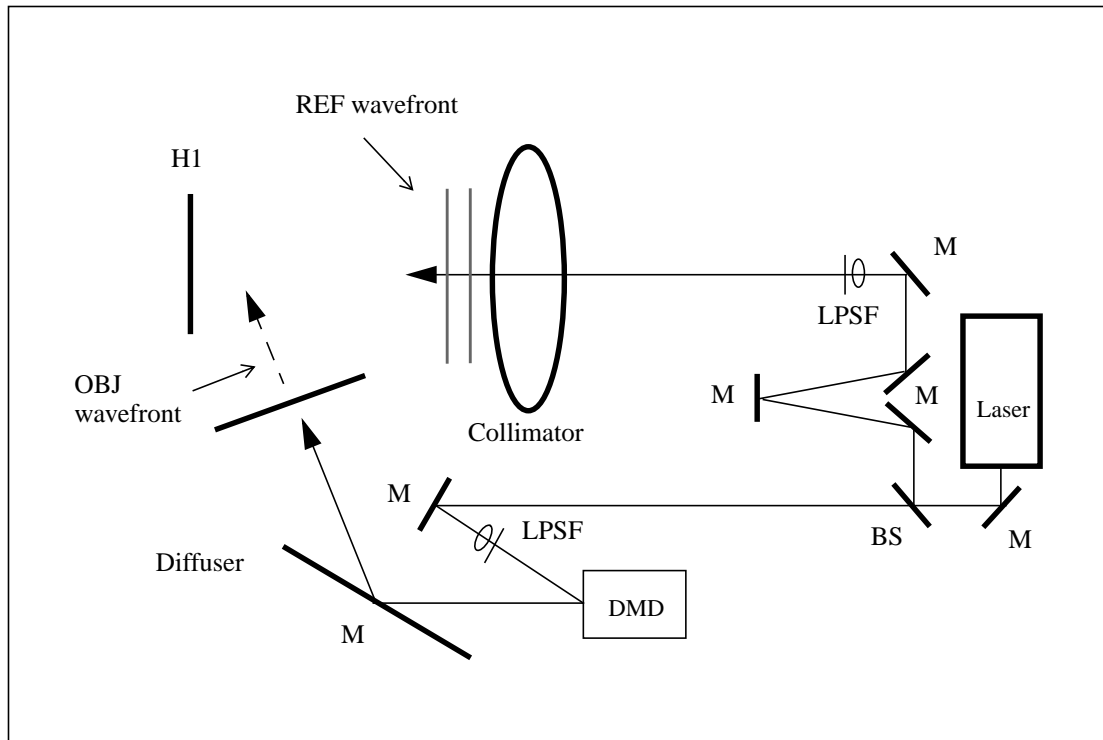


Figure 5.7: Optical setup used for recording a conventional transmission H1 using a digital micromirror device (DMD) to project an image onto a diffuser. (LPSF--lens-pinhole spatial filter; M--mirror; BS--beam splitter)

### *Conventional transmission master (H1)*

A 20.3 x 25.4 cm (8 x 10 in) checkerboard pattern was generated with Adobe Photoshop and Microsoft Powerpoint and projected onto a ground-glass diffuser via a Texas Instruments digital micromirror device (DMD) [28]. A collimated reference beam was directed onto the H1 at a 90° angle. A beam ratio of 7:1 was used to record a 20.3 x 25.4 cm full aperture transmission master. The mastering setup, depicted in Figure 5.7 above, is the same as used for a conventional transmission H1 stereogram master. The master was oriented for phase-conjugate illumination for image reconstruction (Figure 5.8).

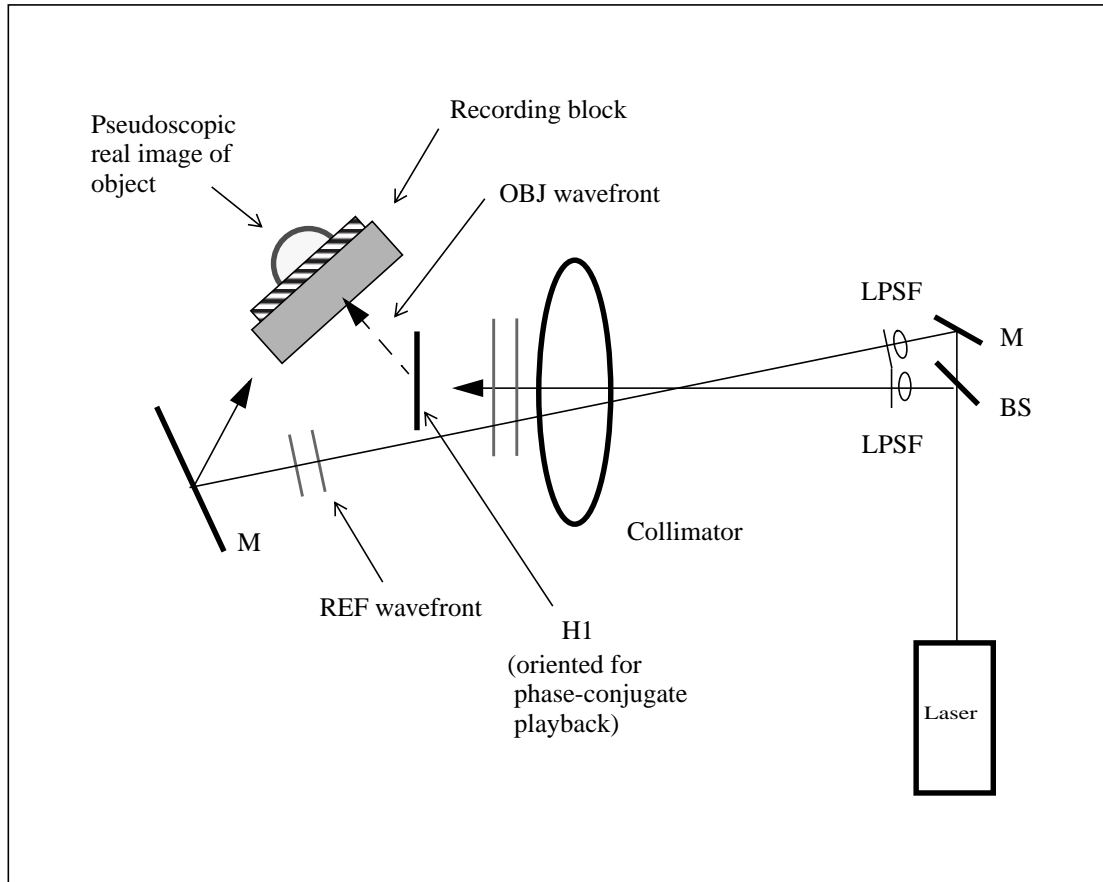


Figure 5.8: Optical setup used to record a transmission-mode edgelit transfer (H2) hologram of a spatial distortion test image. (LPSF--lens-pinhole spatial filter; M--mirror; BS--beam splitter)

### *Edgelit transfer (H2)*

The optical setup used for the edgelit hologram transfer is depicted in Figure 5.8 above. The H2 reference beam was slightly off-axis to the collimator, causing slightly imperfect collimation, but the effects are no worse than experienced with spherical mirror collimators. Also this does not readily allow for path length matching, fortunately the difference is not too great in this setup and is within the coherence lengths of the lasers used. The master was first illuminated as a full-aperture transfer, then later, as a limited-aperture 10 cm slit. The image of the diffuser was positioned onto the back surface of the recording block for transmission-mode recording. A 9x11 inch (23 x 30 cm) photopolymer film sheet

was laminated to the block using a brayer and illuminated with a collimated reference beam at a  $75^\circ$  in-block angle. Beam ratios between 1 and 1.5:1 were tested. Various absorbing materials and film mounting methods were also tested using this optical configuration.

#### *Observations and discussion*

H2's made with a full-aperture H1 had noticeable chromatic blur. Reducing the aperture size to 10 cm reduced blur significantly. The image of the diffuser was reconstructed with few distortion effects or image sway evident--indicating that good phase-conjugate reconstruction was achieved.

Difficulties with lamination led to experimentation with different film mounting techniques. Pre-laminating to an anti-reflection-coated glass plate using a lamination roller setup provided the best film lamination. However, mounting the glass plate to the block (glass to glass), using xylene or immersion liquid, introduced woodgrain. This reinforced the view that direct lamination of the photosensitive layer to the recording block was needed to reduce woodgrain.

### **5.3.3 *Two-step transfer of a three-dimensional object***

#### *Conventional transmission H1*

A 20.3 x 25.4 cm silver-halide full-aperture H1 of the Manta Ray was recorded using the setup and diorama described in Section 5.3.1, Figure 5.4, with the exception that the H1 was located 50 cm from the object. The plate was exposed and processed as normal. The H1 was oriented for phase-conjugate illumination for the transfer step.



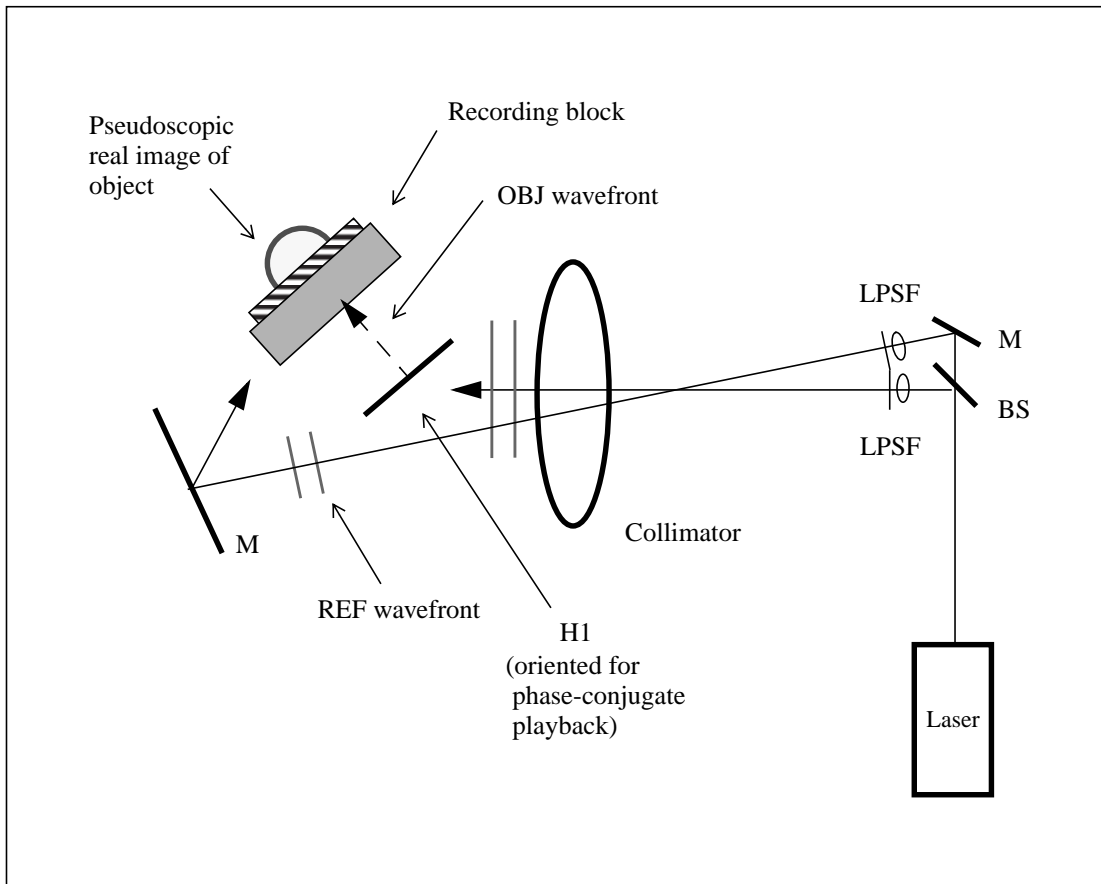


Figure 5.9: Optical setup used to record a transmission-mode edgelit hologram (H2) from a conventional transmission H1 of a three-dimensional object. (LPSF--lens-pinhole spatial filter; M--mirror; BS--beam splitter)

### *Edgelit transfer (H2)*

The optical setup for the edgelit transfer is depicted in Figure 5.9 above. The recording block was positioned to locate the predetermined image plane (2.54 cm from the front of the diorama) of the projected pseudoscopic image of the Manta Ray at the back surface of the block to record a transmission-mode edgelit hologram. A 23 x 28 cm sheet of photopolymer was laminated to the recording block using a silk screen squeegee with a layer of Teflon™ tape affixed to rubber blade to prevent scratching of the film. The reference beam angle used was 75° as measured in the block, and a beam ratio of 2:1 was used.

### *Observations and discussion*

As suspected, the full aperture transfer had fairly bad image blur. Reducing the aperture size to 10 x 25.4 cm produced good quality images that were very bright and had a fairly narrow bandwidth (see Results). Even with this fairly large slit size (compared to conventional transmission holograms) objects deep in the diorama were clear and sharp. The squeegee lamination method solved many of the problems previously mentioned.

## 5.4 Lippmann color technique

Throughout this section and the next, the multi-wavelength beam combining system (described in Section 5.2) was utilized. However, during some of testing, only one or two of the beams were used at a time. The first section describes the use of a conventional multi-wavelength reflection H1 to record color transmission-mode edgelit H2s of diffuse objects. Next, a coupled H1-H2 edgelit recording technique is introduced and used to record one- and full-color holographic diffusers.

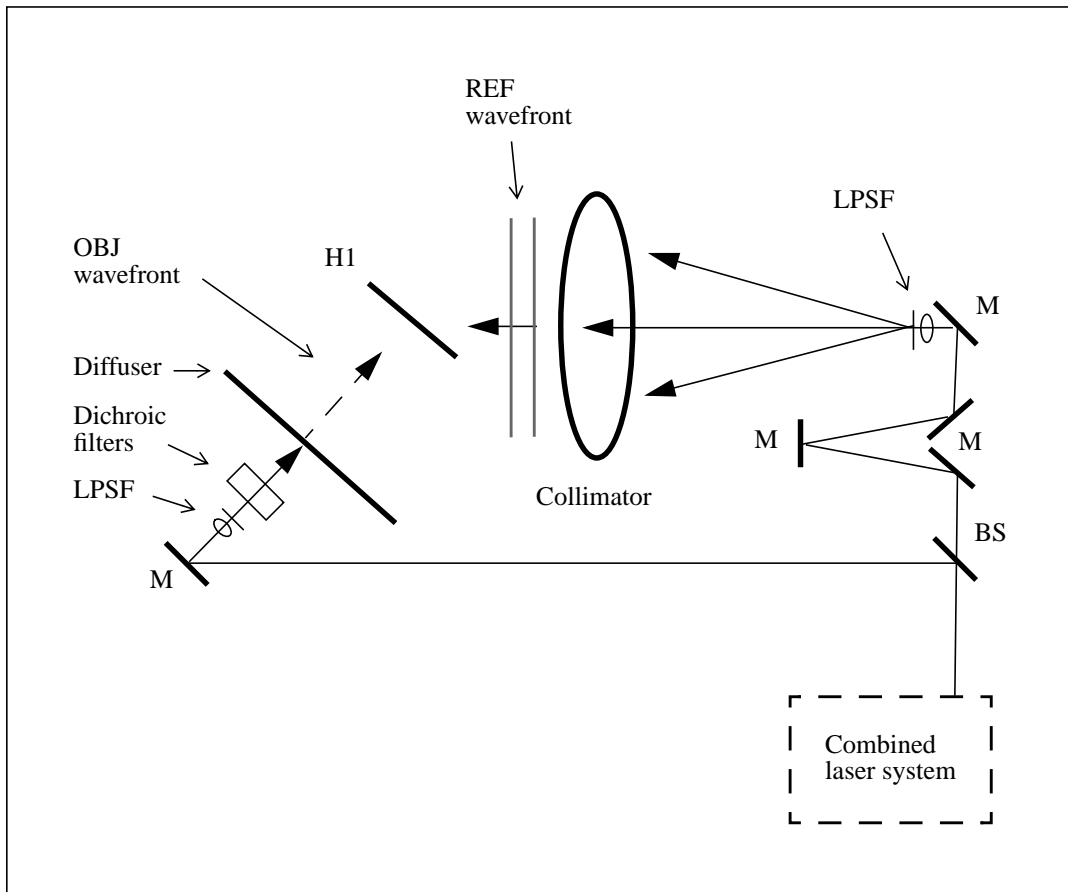


Figure 5.10: Optical setup used to record conventional reflection H1 with two-color gamut. (LPSF--lens-pinhole spatial filter; M--mirror; BS--beam splitter)

#### 5.4.1 Two-color gamut edgelit hologram

##### *Color reflection master (H1)*

Figure 5.10 depicts the optical setup of the reflection H1. Two beams (532 nm and 647 nm) were expanded and directed toward a diffuser at a 90° angle. Two dichroic filters (530 nm and 650 nm) were located in the path of the beam illuminating the diffuser to simulate red and green areas of a color image. The filters needed to be slightly twisted to maximize their throughput for the wavelengths used. Figure 5.11 is a schematic of the image of the diffuser as seen by the recording block.

An open aperture plate holder was located at a  $90^\circ$ , 30 mm from the diffuser. Photopolymer film was laminated directly to 10.2 x 12.7 cm glass plate and oriented in the plate holder with the photosensitive layer toward the object wavefront (Figure 5.12). A collimated reference beam was directed onto the H1 as a  $30^\circ$  angle. A 1.5:1 beam ratio was used, and then the hologram was processed normally.

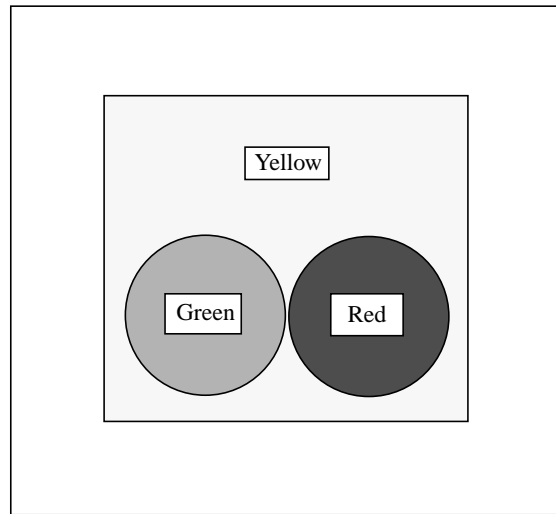


Figure 5.11: Schematic of color test image projected onto diffuser to simulate colored area of an image.

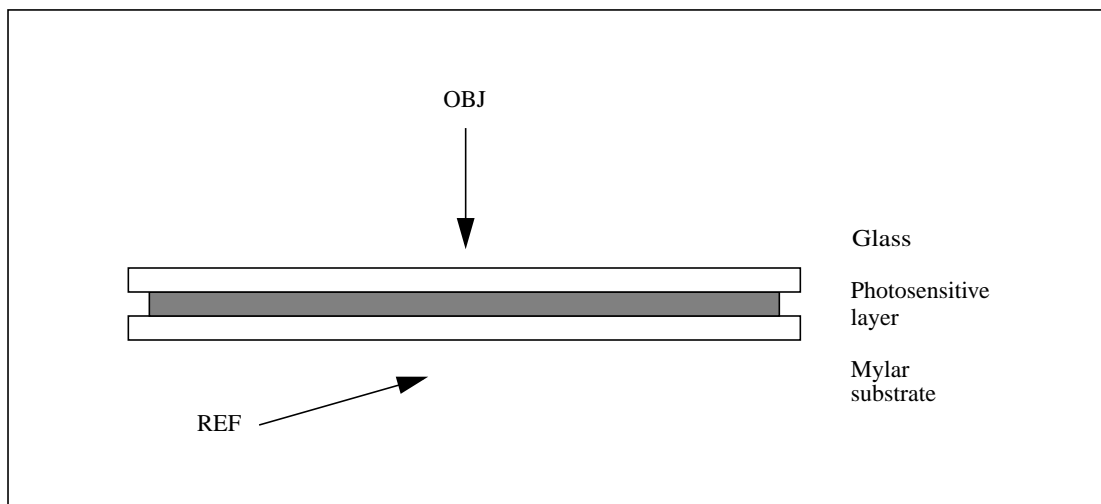


Figure 5.12: Schematic of the coupled recording stack used to record a conventional color reflection H1 in photopolymer.

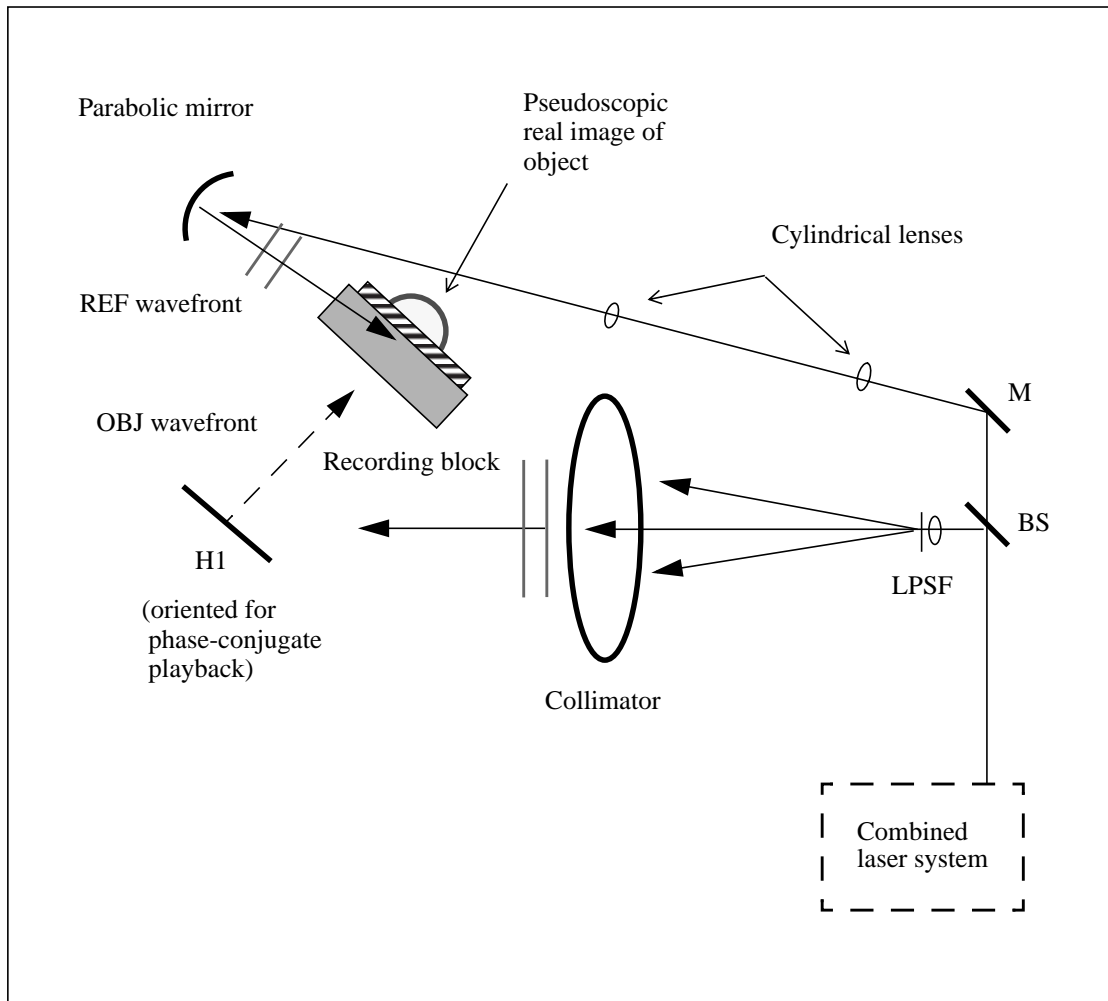


Figure 5.13: Optical setup used to record a color full aperture transfer edgelit hologram using a conventional color reflection H1. (LPSF--lens-pinhole spatial filter; M--mirror; BS--beam splitter)

### *Edgelit transfer (H2)*

The color reflection H1 was oriented for conjugate playback and located as shown in the setup depicted in Figure 5.13. The H2 recording block was oriented for transmission-mode recording. A 10 x 13 cm sheet of photopolymer was laminated directly to the block and a collimated reference beam at a  $75^\circ$  angle in the block was used. The photosensitive layer was exposed at a beam ratio of 1.5:1 and processed normally.

### *Observations and discussion*

The H1 was evaluated in laser light using the wavelength used for recording and white-light. The H1 was very bright and there was a slight shift the Bragg angle due to shrinkage, but the effect was negligible.

The edgelit H2 image was bright but a little bit noisy. This may be due in part to the recording block used in early testing which did not use glass light absorbing material. A double image could be seen which is apparently caused by back reflection of the object light within the block. An anti-reflective coating should help to reduce this effect. For the most part the quality of the image was satisfactory.

### ***5.4.2 Coupled H1-H2 edgelit recording***

#### *Setup and procedure*

As depicted in Figure 5.14, a diffuser was positioned 7 cm from the recording block, and object light was directed onto the diffuser. A large “X” shaped stencil was placed on the surface at the center of the illuminated diffuser area. Images of the diffuser were recorded with this setup using 532 nm light and three-color mixed beams.

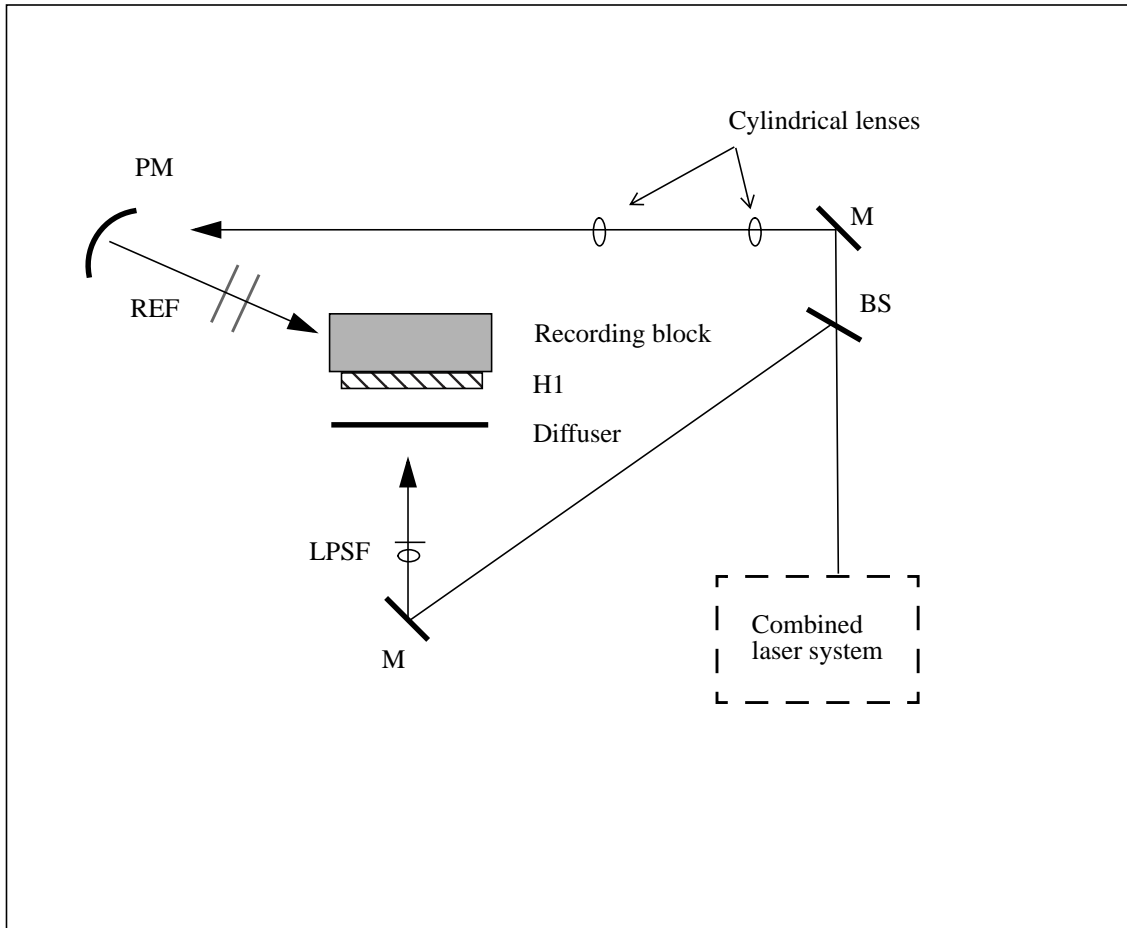


Figure 5.14: Optical recording setup for reflection-mode edgelit master (H1) hologram. (LPSF--lens-pinhole spatial filter; M--mirror; BS--beam splitter)

### *Reflection-mode edgelit master (H1)*

To record a reflection-mode edgelit hologram, the photopolymer recording material is positioned on the side of the block closest to the object as is shown in Figure 5.15. A collimated reference wavefront was directed onto the photosensitive layer at a  $105^\circ$  angle. the photopolymer material was pre-laminated to a piece of anti-reflection coated glass and index matched to the recording block. Exposure and processing were as normal. The H1 was oriented for phase-conjugate image reconstruction and index matched onto the block using index matching fluid (Figure 5.16) for the transfer step.

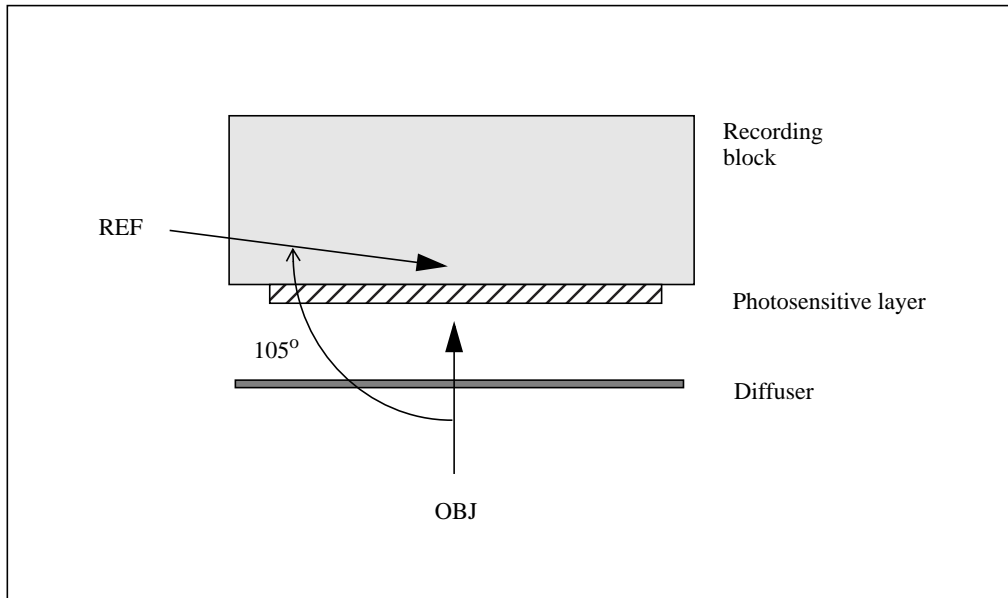


Figure 5.15: Optical recording setup for reflection-mode edgelit master (H1). Note that the distance between the diffuser in-air is less than the block thickness due to the effects of refraction. (The photosensitive layer substrate and light absorbing materials are not shown.)

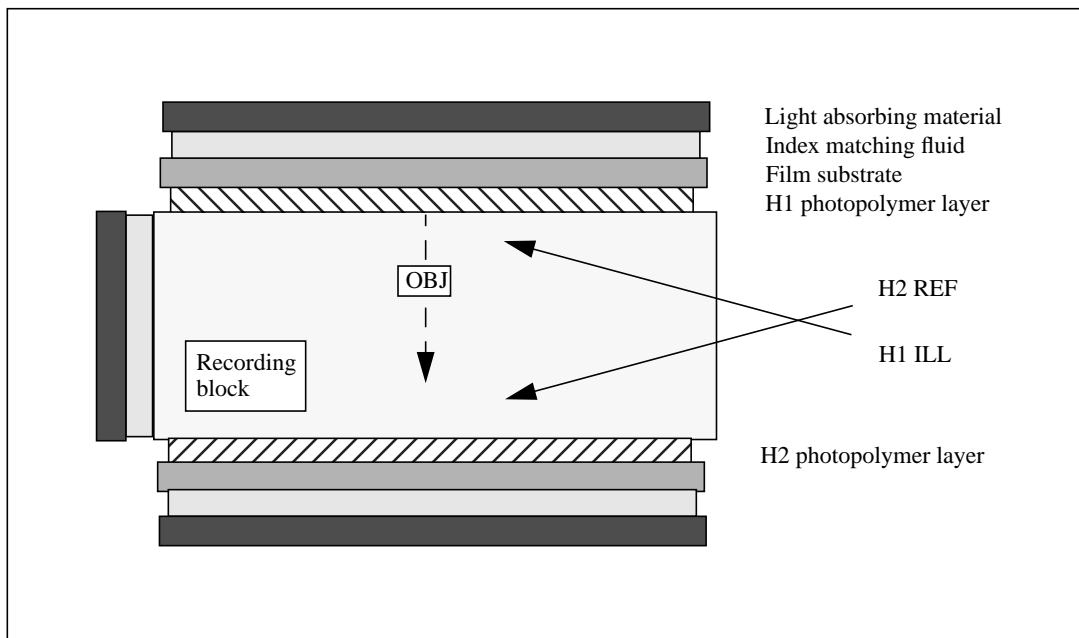


Figure 5.16: Detail of typical recording stack used to record a transmission-mode edgelit transfer hologram using a reflection-mode edgelit H1 coupled to the same recording block.



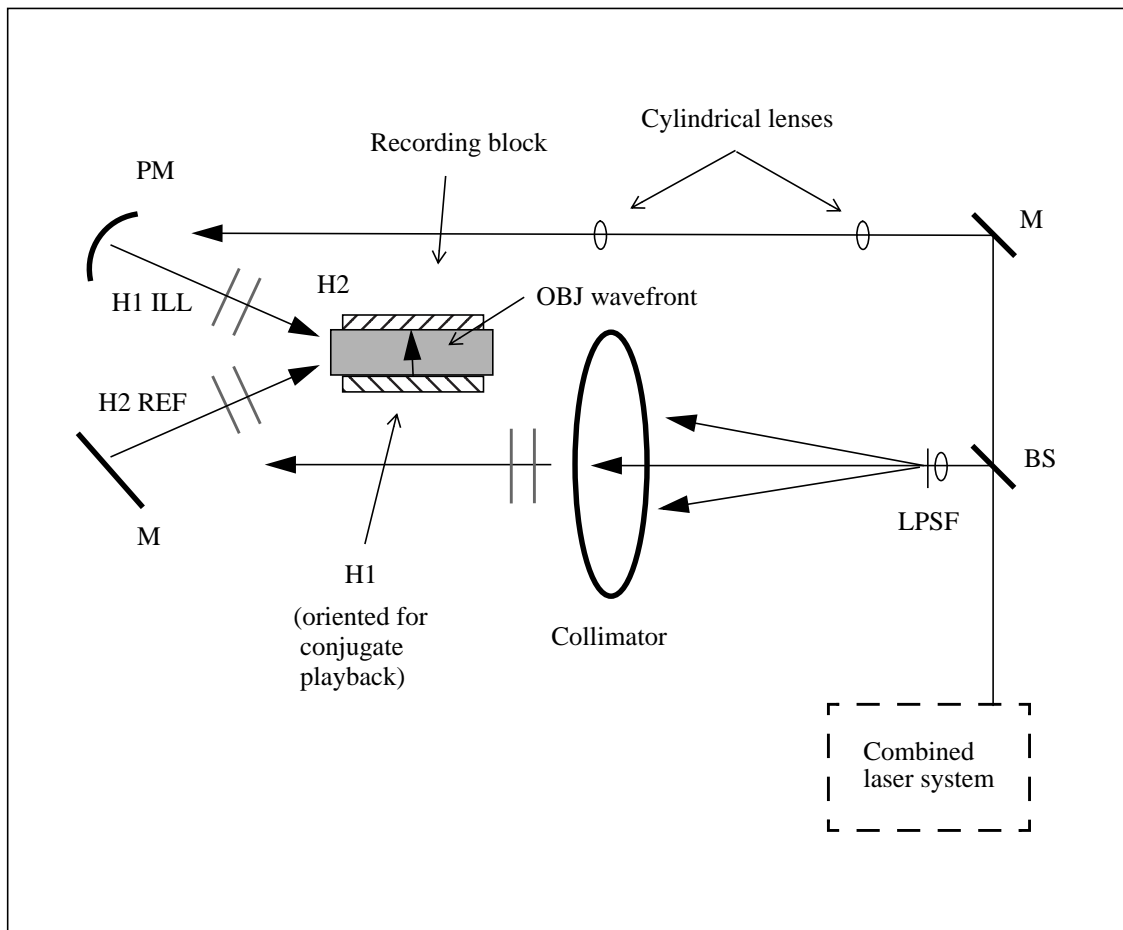


Figure 5.17: Optical setup used for recording a transmission-mode edgelit (H2) hologram using an edgelit reflection H1 coupled to the same recording block. (LPSF--lens-pinhole spatial filter; M--mirror; BS--beam splitter)

### *Color edgelit transfer hologram (H2)*

As depicted in Figure 5.16, the photopolymer was laminated (photosensitive layer toward the block) opposite the H1 on the recording block--as for a normal transmission-mode edgelit hologram. The H2 reference beam was directed onto the photosensitive layer at a  $75^\circ$  angle in the transfer setup, and the H2 exposed and processed normally.

### *Observations and discussion*

The reflection-mode H1s recorded using the normal film application method (laminating

the photosensitive layer directly to the recording block) had noticeable surface fringing (woodgrain) after processing and re-application to the block (in phase-conjugate reconstruction).

Attempts to record holograms with the photosensitive layer toward the object beam resulted in woodgrain induced by the additional interface caused by index matching liquid needed to couple the film to the block. A solution to this problem might be found by using DuPont mastering film, such as, HRF-750X131-20, which is designed to allow removal of the cover sheet from both sides of the photopolymer. With this film, the birefringent layers can be completely removed from the optical path. However, at the time of writing, this theory has not been tested.

Regardless of the woodgrain-like problems observed, three-color reflection edgelit H1s of a diffuser were recorded, reconstructed in phase-conjugate, and transferred into transmission-mode edgelit H2s using this block recording method.

## 5.6 Results

### 5.6.1 *Woodgrain reduction using photopolymer*

Woodgrain was recognized early on as a major problem which affecting the edgelit recording technique [3, 5, 25, 39]. Utilization of DuPont's photopolymer recording material immediately reduced the woodgrain problem. This is related in-part or whole to the direct application of the photosensitive layer to the block, and may be further aided by the self-induced index matching phenomena described by Phillips *et al.*[31] and Coleman *et al.* [8]. Solving this problem is the first step to recording acceptable edgelit display holograms, and DuPont's photopolymers have helped solve woodgrain problems in the research reported here.

### 5.6.2 *PMMA and photopolymer incompatibility*

It had been expected early on, that PMMA would prove to be a good material for the recording block. Unfortunately, when the PMMA block tested here was coupled to photopolymer materials the author discovered unsettling side effects. Bright images could not be obtained using the PMMA block; and often the photopolymer would delaminate from its substrate. Fortunately, the glass recording block which was fabricated worked very well, and was found to be the best material for use as a recording block.

The dim images observed when recording on PMMA were not caused by the vibrational stability of the system. This was verified by slightly rotating the recording block so as to obtain a steep-angled external reference beam (all other components were left in place), and recording a conventional reflection hologram. The hologram was bright and essentially normal, implying the problem originated with the PMMA block. The following sections offer some theories that may explain PMMA's poor performance.

#### *Thermal expansion*

PMMA is a soft material which expands and contracts with temperature change. According to PMMA manufacturer Polycast [29], their material expands  $\sim 400\text{nm} / 1\text{ cm}$  for each  $1^\circ\text{F}$  increase in temperature. Thus, a block 25.4 cm long will increase  $10.2\ \mu\text{m}$  in length given a  $1^\circ\text{F}$  temperature increase. As we know, if the reference or object path lengths change (relative to each other) one quarter of a wavelength (133nm in case of a 532 nm recording wavelength) fringe contrast will be degraded a dim hologram will be the result. In this setup, if the temperature changes in excess of  $0.013^\circ\text{F}$  during the exposure, the block may expand enough to cause a dim hologram.

Phase change caused by thermal expansion of optics is a commonly observed phenomena when using high-powered short wavelength lasers and long exposure times typical of photoresist mastering. Optics in the optical path heat up and expand during exposure requiring active fringe locking to compensate for the effects. In the experiments undertaken here, the 100mW laser used has more than twice the power of those used by Birner [5] and Henrion[15], and its shorter wavelength packs more energy. These factors, coupled

with much longer exposure times (in some cases one-hundred times longer than necessary for silver-halide materials) may explain why other researchers did not report being affected by this phenomenon.

#### *Chemical reaction*

The other detrimental effect noted when using PMMA was the delamination (and destruction) of the photosensitive layer from the substrate after exposure. Overexposing the material would sufficiently hardened it so as to facilitate release from the block, but this is an undesirable solution. Mike Klug, in a personal conversation with the author, suggested that the monomers in DuPont's photopolymer material may act as a solvent to bond it to the PMMA recording block. This factor, monomer migration into the PMMA recording block, may also be a cause for the dim imagery observed. A hard-coat on the PMMA material may solve this problem, but this was not tested.

#### *Birefringence and striations*

When the recording block is illuminated with monochromatic light, striations (caused by birefringence) can be observed near the major faces. Most plastics are slightly birefringent. PMMA is considered better than most; however, at the steep grazing angles used for edgelit holography, the light must travel through a lot of material before reaching the photosensitive layer. It is possible a little bit of birefringence does a lot of harm in the edgelit hologram geometry.

### **5.6.3      *Scaling and collimation***

Collimation of the reference beam was a key factor that enabled scaling up the size of the edgelit holograms reported in this research. One of the main problems in scaling edgelit holograms, non-uniformity of the reference beam irradiance profile, was alleviated because the collimating lens system provided enough distance from the source to allow an average irradiance variation of 10% in horizontal direction (across the recording block's edge, x-axis) and 5% in the vertical direction (z-axis). A direct diverging playback method would not be able to attain this level of variation without at least a meter of distance between the light source and the block (which would make the display stand far from

compact), or by attenuating the illumination light to remove the brightest areas of the beam profile, which would lower the overall brightness of the display.

As predicted in Section 4.2.1, three-dimensional spatial and chromatic distortions were also avoided by the use of a non-diverging collimated wavefront. In the largest edgelit holograms (20.3 x 25.4 cm), there was slight image sway, but this can be attributed to either imperfect collimation by the diverging collimating lens used and/or by imperfect phase-conjugation. The spectral dispersion was, as measured by eye, limited to one axis. The factors listed above, and the fact that collimation enables straightforward phase-conjugation of transfer (H2) holograms show that this technique is can be very useful for edgelit holography.

#### **5.6.4 *Two-step transfers via phase-conjugation***

As described above, edgelit holograms illuminated in phase-conjugate demonstrated no obvious adverse effects or major problems when applied to the edgelit format. Applying this technique to the edgelit hologram enables the use of conventional stereogram and three-dimensional object recording techniques. Furthermore, by eliminating the intermediate master (H2) in the three-step technique, the image viewzone is increased, and production time and money are saved. Finally, this technique enables the application of a coupled H1-H2 edgelit recording technique.

#### **5.6.5 *Coupled H1-H2 edgelit recording***

This technique has demonstrated promise for two-step master-transfer edgelit holography. However there are some technical difficulties that still need to be solved. The direct application of the photopolymer to the recording block (which normally solves woodgrain problems) was not conducive to good fringe contrast when used to record a reflection-mode edgelit. The reason for this may be explained as follows. Polarization of the light emanating from the diffuser is slightly scattered. As the object light passes through the birefringent polyester substrate of the film, polarization is affected even more, causing loss

of fringe contrast in local areas of the photosensitive layer and a surface fringing effect (similar to woodgrain) which affects image quality. When the image is transferred from the H1 to the H2, this effect causes the H2 hologram to have non-uniform irradiance across the image area.

The root of this problem is most likely related to the birefringence of the polyester substrate, and its biaxial characteristics (the polarization axis of this material is different for each of its  $x$ ,  $y$ , and  $z$  axes, so matching the predominant polarization axis of the substrate with the polarization axis of the reference and object beams is a challenge). Simply removing the substrate completely from the optical system, by using DuPont's photopolymer mastering films, may solve this problem. This problem was not completely solved in this research; however, monochromatic and full-color holographic diffusers were recorded using this technique. Aside from a slight mottled irradiance uniformity, there did not appear to be any other problems or distortions inherent to this technique which would limit its future development.

### **5.6.6**      *Color*

For evaluation, holograms were placed onto the display stand (Section 4.3.2) for illumination. Bandwidth was determined by measuring the full width of the diffraction efficiency profile at 50% of the maximum diffraction efficiency using dichroic filters with 10 nm increments. The output characteristics of the illumination source were not taken into account for the measurements reported here.

#### *One wavelength recording*

The bandwidth of the transmission-mode edgelit holograms recorded with one wavelength averaged 70 nm, which is close to the values predicted by Leith *et al.*[23], and obtained by Henrion (Section 2.2.5, Table 1). However, the bandwidth was slightly higher than expected, given the thicker recording material used here. This could be caused by inaccuracy in the bandwidth measurement technique used, or by the characteristics of the photopolymer recording material.

The edgelit holograms made with collimated reference and illumination beams, dispersed light evenly along the  $y$ -axis, and did not indicate any noticeable chromatic distortions. Furthermore, they did not show any substantial lack of blue wavelength light. Bandwidth was essentially centered about the recording wavelength (532 nm), and encompassed a 490-560 nm range.

As noted by Ueda *et al.* [36], image blur of edgelit holograms can be reduced by utilizing an rainbow (slit) master hologram. The transmission-mode H2s made using a conventional transmission slit master, allowed for a slightly larger aperture size (and more parallax information) than would ordinarily be used for a conventional rainbow hologram, but not enough for a full-aperture transfer. As suggested by Ueda *et al.*, a thicker recording layer (they recommend 29  $\mu\text{m}$ --twice as thick as the 15  $\mu\text{m}$  thick material used here) will help achieve better wavelength selectivity and should allow recording of full-color full-aperture transfers of imagery using white-light illumination.

#### *Multi-wavelength recording*

The transmission-mode edgelit holograms made here using three-wavelengths had a total bandwidth of about 220 nm, encompassing a color gamut of wavelengths between 660-440 nm. This the individual colors are slightly too broad-band to achieve accurate color selectivity for most imaging applications; however, they should prove acceptable for use as diffusers in applications such as, LCD back-light illumination, or real-time display.

Broadband white-light source illumination is not recommend for reconstruction of full-color imagery with full-parallax using the techniques reported here. However, if narrow-band light sources, i.e., laser diodes or light emitting diodes (LED), were used, these holograms can be reconstructed with better wavelength selectivity and image blur characteristics. Diode illumination was investigated over the course of this research, and provided a reduction in color blur which allowed reconstruction of deep imagery with little color blur. Unfortunately, the diode source used was found to be not bright enough for use in the display stand. However, brighter red, green and blue diode sources are continually becoming available and could prove valuable as mixed wavelength illumination sources for edgelit holography in future work.

### 5.6.7 *Image qualification*

Imagery was evaluated in terms of brightness, contrast and irradiance uniformity. For evaluation, holograms were placed onto the display stand (Section 4.3.2) for illumination, and irradiance was measured using a Minolta Spotmeter.

#### *Two-step rainbow transfer hologram*

Figure 5.18 is a digital photograph of the 20 x 25 cm monochromatic two-step transfer hologram (H2) described in Section 5.5.3. The H2 was mounted to a 25.4 x 25.4 x 5 cm PMMA block using index matching fluid. The brightest spot on the image measured 30 foot-Lambert; the contrast ratio (brightest:background) was found to be 19:1. The image displayed smooth irradiance variation in the continuous-tone areas of the object.

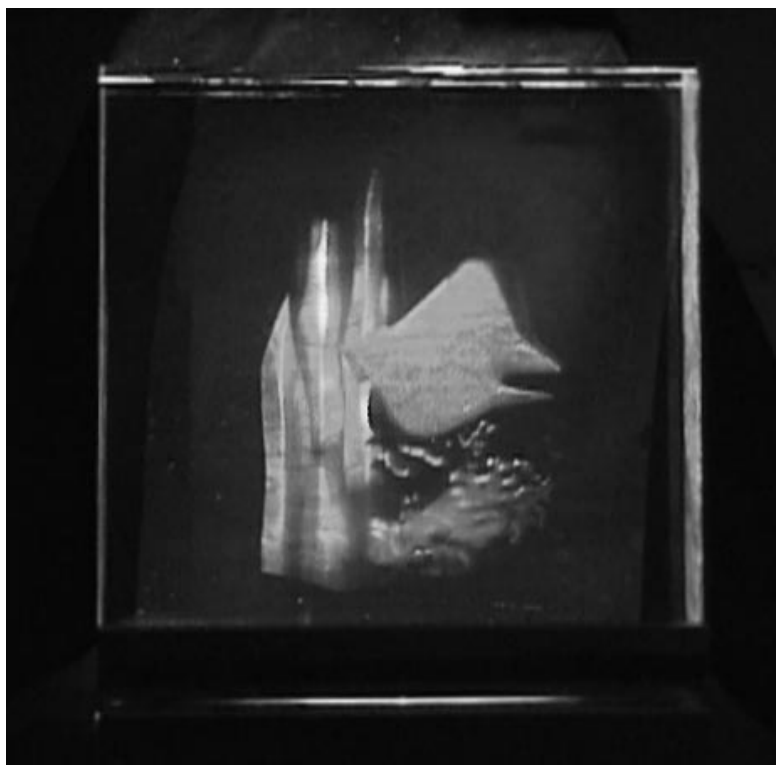


Figure 5.18: Digital photograph of the 20 x 25 cm monochromatic two-step transfer hologram (H2) (Section 5.5.3). The H2 was recorded using a conventional transmission master (H1) with a 10 x 254 cm aperture.



There was a problem observed, which is apparently introduced by the transmission-mode recording technique, that causes a dim double image of the object to be recorded. During recording, object light passes through an air/recording block interface prior to exposing the photosensitive layer (Figure 4.5). This light is back-reflected by the recording stack/air interface, and again at the first interface. This causes a double image of the object to be recorded, which is visible upon reconstruction. A technique suggested by Benton (in personal conversation) may solve this problem. It involves index matching a light absorbing material onto the front (object side) face of the block to absorb this back-reflected light. This technique may reduce the effect, but it was not tested here.

#### *Multi-color diffusers*

The following diffusers were recorded using the coupled H1-H2 technique (Section 5.4.2). The average brightness of the transmission-mode edgelit transfer (H2) diffuser made with a single wavelength (532 nm) laser beam was 17 foot-Lambert. A contrast ratio of 11:1 was obtained.

The diffusers recorded with three-wavelengths had a brightness of 50 foot-Lambert, but the contrast was only about 5:1 (the hologram was overexposed somewhat). As mentioned above (Section 5.6.5), the problems encountered obtaining uniform irradiance profile caused slight mottling of the light output distribution of the H1. This effect is mitigated slightly in the transfer step, but it is still noticeable. There needs to be more development work undertaken to eliminate this problem.

#### **5.6.8**      *Summary of results*

DuPont's new photopolymer recording materials reduced the effects of woodgrain in the block recording geometry primarily because the surface tension of the photopolymer allows direct application of the photosensitive layer to the block. However, the interaction between the photopolymer's monomers and PMMA (and other physical characteristics of PMMA) caused many problems, resulting in the abandonment of PMMA as a recording block. BK-7 glass was found to be a superior material, and provided robust recording block.

Collimation and phase-conjugation were key factors for enabling the size increase of the edgelit holograms made here. Collimation helped reduce irradiance non-uniformity, spatial and chromatic distortions, and enabled the use of phase-conjugate image reconstruction techniques. In turn, phase-conjugate image reconstruction allowed the use of standard two-step recording techniques to achieve edgelit holograms of a three-dimensional object without the usual intermediate master. Furthermore, collimation and phase-conjugate reconstruction methods enabled development of a coupled edgelit H1-H2 recording technique which provides a simple method of transferring edgelit holograms. However, it must be noted that problems are caused by the birefringent (and biaxial) polyester substrate of DuPont's photopolymer material when recording the reflection-mode edgelit H1 needed for this technique. Although, there are other recording materials available from DuPont which may solve this problem.

Color control was also facilitated by the use of a collimated reference beam. Light was dispersed by the transmission-mode edgelit holograms uniformly over the vertical axis and had a fairly narrow bandwidth (compared to a conventional transmission hologram). This suggests that good color registration using rainbow color mixing techniques can be achieved. However, the bandwidth measured here indicated that Bragg color selection characteristics are not adequate for providing Lippmann color control using white-light illumination sources. However, the bandwidth should be adequate if narrow-band mixed-color illumination sources are used for illumination.

# Chapter 6

## Conclusion

This research has extended the size capability of the edgelit display holograms by producing 20.3 x 25.4 cm (8 x 10 in) images which are 400% larger than previously reported. Collimated reference/illumination beam, and phase-conjugate image reconstruction techniques were developed and utilized to obtain the results of this research. Two-step transfer edgelit holograms of diffusers and a three-dimensional objects were recorded using conventional transmission H1s; and full-color and narrow-band holographic diffusers were also recorded using conventional reflection, and reflection-mode edgelit H1s.

DuPont's photopolymer has proven to be a great asset when used for the edgelit holography reported here. The surface tension of this material allowed direct application of the photosensitive layer to the recording block and virtually eliminated the woodgrain effects which have plagued the edgelit technique since its invention. Furthermore, the panchromatic characteristics of this material has produced bright full-color edgelit holograms, and offers encouragement for the future of edgelit holography.

The decision to use a collimated wavefront for the reference beam was key factor for increasing the size of the edgelit hologram's imaging capability. Collimating the reference and illumination light reduces the irradiance non-uniformities which affect direct diverging-source illumination techniques when image size is scaled up. The distance required to

collimate the illumination light for the display stand is increased (over direct illumination methods), and the optics needed to collimate the illumination beam increases the cost of the display stand, but these factors are balanced by the benefits realized by collimation.

Collimation also allows convenient phase-conjugate illumination of edgelit holograms. The ability to correctly illuminate edgelit holograms in phase-conjugate enables the production edgelit transfer holograms of three-dimensional objects in two-steps instead of the usual three. Another technique developed during the course of this research is a coupled H1-H2 recording method which allows for a compact, vibrationally-stable, and efficient transfer hologram recording method. This technique can prove useful for the mass-production of edgelit holographic stereograms and diffusers.

## 6.2 Future work

Several practical problems have plagued conventional reflection and transmission holography since their invention. These include the need for a special external light source, and the image blurring due to the size of typical sources and extraneous light in the display environment. The compact illumination geometry and small footprint of edgelit hologram displays have been shown to reduce the effects of those problems, but several other problems remain, such as the attainment of images in sizes useful for practical displays and full-color images with full-parallax information.

This research has demonstrated that edgelit holograms can be scaled up to sizes of current interest for display holography by the use of simple but careful techniques, and that new DuPont photopolymer recording films reduce improve image quality (by reducing woodgrain) and make possible full-color edgelit holograms at that size.

There are still many problems to overcome. For example, the size of edgelit holograms must be increased still further to meet the growing expectations of the display market, and the attainment of full-color images with full-parallax is needed. Holographic

diffusers are finding increasing use in display applications as liquid crystal display (LCD) illuminators. Development of low-cost full-color edgelit holographic LCD illuminators could prove to be very useful to the display industry. Solving these problems will require much work, and perhaps still newer techniques for hologram recording. Once those questions are answered, the extension of the edgelit technique to holographic stereograms, pulsed-laser imaging, and real-time displays will follow.

When large-area, full-color edgelit display holograms are at last made available to the public, perhaps the imaging potential of this medium will be realized and holography will become an accepted tool for scientific, architectural and commercial displays.

# Bibliography

- [1] S.A. Benton, "Hologram reconstruction with extended light sources," *J. Opt. Soc. Am.* **59**, p.1545A (1969).
- [2] S. Benton and S. Birner, "Self-contained compact multi-color edge-lit holographic display," *U.S. Patent 5,121,229*, June 9 1992 (filed August 9 1989).
- [3] S. Benton, S. Birner, and A. Shirakura, "Edge-lit rainbow holograms," *SPIE Proceedings Vol. 1212*, p.149 (1990).
- [4] S. Benton, *MAS450 Class Notes*, version 9/97.
- [5] S.M. Birner, "Steep reference angle holography: Analysis and Applications," Master's thesis, Massachusetts Institute of Technology (February 1989).
- [6] H. Bjelkhagen, *Silver-halide recording materials for holography and their processing*, Springer series in optical sciences Vol. 66, Springer-Verlag Berlin Heidelberg (1993).
- [7] H. I. Bjelkhagen and T.H. Jeong "Recording and processing of silver-halide color holograms," *SPIE Proceedings Vol. 2405*, p.100 (1995).
- [8] Z. Coleman *et al.*, "Holograms in the extreme edge illumination geometry," *SPIE Proceedings Vol. 2688* (1996).
- [9] Y. Denisyuk, "Photographic reconstruction of the optical properties of an object in its own scattered radiation field," *Sov. Phys. Docl.* **7**, p.543 (1962).
- [10] W.J. Farmer et al., "The application of the edge-lit format to holographic stereograms," *SPIE Proceedings Vol.1461*, p.171 (1991)
- [11] W.J. Farmer, "Edge-lit holographic stereograms," Master's thesis, Massachusetts Institute of Technology (June 1991).
- [12] D Gabor, "A new microscopic principle," *Nature* **161**, p.777 (1948).
- [13] W.J. Gambogi *et al.*, "Color holography using DuPont holographic recording films," *SPIE Proceedings Vol. 2405*, p.62 (1995).
- [14] M. Halle, "The Ultragram: a generalized holographic stereogram," *SPIE Proceedings Vol. 1461* (1991).
- [15] M. Henrion, "Diffraction and exposure characteristics of the edgelit hologram," Master's thesis, Massachusetts Institute of Technology (September 1995).
- [16] Q. Huang and H. Caulfield, "Waveguide holography and its applications," *SPIE Proceedings Vol. 1461*, p.303 (1991).

- [17] P. Hubel and L. Solymar, "Color-reflection holography: theory and experiment," *Applied Optics* **30**, p.4190 (1991).
- [18] N. Kihara, "One-step edge-lit transmission holographic stereogram printer," *SPIE Proceedings Vol. 3637*, p.2 (1999).
- [19] H. Kogelnik, *Guided-wave optoelectronics*, Tamir ed., 2nd edition, Springer-Verlag Berlin-Heidelberg (1990).
- [20] T. Kubota, "Recording of high quality color holograms," *Applied Optics* **25**, p.4141 (1986).
- [21] T. Kubota, "Method for reconstructing a hologram using a compact device," *Applied Optics* **31**, p.4734 (1992).
- [22] E. Leith and J. Upatnieks, "Wavefront reconstruction with continuous-tone objects," *J. Opt. Soc. Am.* **53**, p.1377 (1963).
- [23] E. Leith, *et. al.*, "Holographic data storage in three-dimensional media," *Applied Optics* **5**, p.1303 (1966).
- [24] L. H Lin and C.V. LoBianco, "Experimental techniques in making multicolor white light reconstructed holograms," *Applied Optics* **6**, p.1255 (1967).
- [25] L. H. Lin, "Edge-illuminated hologram," *J. Opt. Soc. Am.* **60**, p.714A (1970).
- [26] G. Lippmann, "Sur la theorie de la photographie des couleurs simples et composees par la methode interferentielle," *J. Phys. (Paris)* **3**, p.97 (1894).
- [27] V. Markov and A. Khizhnyak, "Selective characteristics of single layer color holograms," *SPIE Proceedings Vol. 2652*, p.304 (1996).
- [28] R. Nesbitt *et al.*, "Holographic recording using a digital micromirror device," *SPIE Proceedings Vol. 3637*, p.12 (1999).
- [29] Personal communication with Angelo Lacasello of Polycast Corp.
- [30] N.J. Phillips and W. Ce, "The recording and replay of true edge-lit holograms," *IEE Conference Publication 342*, p.8 (1991).
- [31] N.J. Phillips *et al.*, "Holograms in the edge-illuminated geometry - new materials developments," *SPIE Proceedings Vol. 1914*, p.75 (1993).
- [32] G. Saxby, *Practical Holography*, Prentice Hall, New York, XXX.
- [33] S. Stevenson, "DuPont multicolor holographic recording films," *SPIE Proceedings Vol. 3011*, p.231 (1997).
- [34] Y. Taketomi and T. Kubota, "Deep image reconstruction of a reflection hologram using a fluorescent lamp," *SPIE Proceedings Vol. 3293*, p.196 (1998).

- [35] H. Ueda *et al.*, "Edge-illuminated color holograms," *SPIE Proceedings Vol. 2043*, p.278 (1994).
- [36] H. Ueda *et. al.* "Image blur of edge-illuminated holograms," *Optical Engineering* **37(1)**, p.241 (1998).
- [37] J. Upatnieks, "Method and apparatus for recording and displaying edge-illuminated holograms," *U.S. Patent 4,643,515*, February 17 1987.
- [38] J. Upatnieks, "Compact holographic sight," *SPIE Proceedings Vol. 883*, p.171 (1988).
- [39] J. Upatnieks, "Edge-illuminated holograms," *Applied Optics* **31**, p.1048 (1992).
- [40] J. Walker and S.A. Benton, "In-situ swelling for holographic color control," *SPIE Proceedings Vol. 1051*, p.192 (1989).
- [41] A. Ward *et. al.*, "Total internal reflection holograms--what is new?" *SPIE Proceedings Vol. 600*, p.57 (1985).